


Article

Phosphorus Threshold for the Growth of *Microcystis wesenbergii*, *Microcystis aeruginosa*, and *Chlorella vulgaris* Based on the Monod Formula

Yansen Guo, Wenrui Fu, Nan Xiong, Jian He * and Zheng Zheng * 

Department of Environmental Science and Engineering, Fudan University, Shanghai 200433, China; 21210740051@m.fudan.edu.cn (Y.G.); 18307110491@fudan.edu.cn (W.F.); 22210740079@m.fudan.edu.cn (N.X.)

* Correspondence: hejian@fudan.edu.cn (J.H.); zzhenghj@fudan.edu.cn (Z.Z.)

Abstract: The outbreak of algae in freshwater bodies poses an important threat to aquatic ecosystems, making finding an effective method for controlling algal blooms imperative. Numerous key factors influence algal bloom outbreaks, with nutrient levels in the water body being the decisive factor. Current research regarding the effect of nutrient levels on algal growth shows that phosphorus is a nutrient that influences algal blooms. Herein, we propose the concept of a modified Monod model for the relationship between algal specific growth rate and phosphorus concentration. Through this improved Monod model, we inferred that the phosphorus concentration at a specific growth rate of zero is the lower threshold of phosphorus concentration that limits algal growth and can effectively control algal outbreaks. This lower threshold is denoted as S' . On the basis of this concept, we designed algal growth experiments. Our results provided an equation that effectively describes the relationship between algal growth and nutrient concentration. When three algal species grow under phosphorus-limited conditions, the corresponding phosphorus concentrations at which they maintain a growth rate of 0 are 0.0565, 0.0386, and 0.0205 mg/L as reflected by the following order of their S' values: *Microcystis wesenbergii* $S' < Microcystis aeruginosa$ $S' < Chlorella vulgaris$ S' . Furthermore, with the increase in phosphorus concentration, the growth of *M. aeruginosa* becomes faster than that of *M. wesenbergii* and *C. vulgaris*. Consequently, *M. aeruginosa* becomes the dominant population in the water, leading to its predominance in algal blooms. This situation explains the common occurrence of cyanobacterial blooms. Our findings provide a theoretical basis for regulating the concentration of phosphorus to control algal outbreaks. Therefore, our study is of great importance for controlling the eutrophication of water bodies.

Keywords: algae; phosphorus threshold; phosphorus deficiency condition; modified Monod model



Citation: Guo, Y.; Fu, W.; Xiong, N.; He, J.; Zheng, Z. Phosphorus Threshold for the Growth of *Microcystis wesenbergii*, *Microcystis aeruginosa*, and *Chlorella vulgaris* Based on the Monod Formula. *Water* **2023**, *15*, 4249. <https://doi.org/10.3390/w15244249>

Academic Editors: Jieming Li and Hong Li

Received: 3 November 2023

Revised: 5 December 2023

Accepted: 8 December 2023

Published: 12 December 2023



Copyright: © 2023 by the authors. Licensee MDPI, Basel, Switzerland. This article is an open access article distributed under the terms and conditions of the Creative Commons Attribution (CC BY) license (<https://creativecommons.org/licenses/by/4.0/>).

1. Modified Monod Model and Its Significance

The introduction of large quantities of nitrogen, phosphorus, and other nutrients into stagnant water bodies can lead to eutrophication and trigger algal blooms, particularly those involving harmful species, such as cyanobacteria, with far-reaching and detrimental effects on aquatic ecosystems. The harmful algal bloom toxins produced during these blooms pose considerable risks to aquatic life, causing fish kills and poisoning various organisms. Additionally, these toxins can jeopardize human health through the consumption of contaminated water or aquatic organisms [1]. Therefore, effectively controlling the occurrence of algal blooms is crucial. Several factors influence algal outbreaks [2,3], with nutrient levels in the water playing a decisive role [4] and affecting the biomass and net productivity of algae [5]. Nutrient supply not only influences the synthesis of algal ATP [6,7], it also affects protein composition [8]. Among nutrients, nitrogen and phosphorus are considered crucial factors affecting cyanobacterial bloom outbreaks [9–12]. A case study using the water quality data of Lake Taihu from the past decade found that the annual average concentrations of total nitrogen (TN) and total phosphorus (TP) in

Lake Taihu fluctuated from 1.26 mg/L to 2.43 mg/L and from 0.060 mg/L to 0.103 mg/L, respectively. The nitrogen-to-phosphorus ratios in the aquatic ecosystems of major lakes in China often exceed 16. Research on Dianchi Lake [13] indicated the importance of controlling phosphorus concentration in the water. By drawing on the research of Redfield et al. [14] and Liebig's law of the minimum, [15] this study proposes the exploration of a lower phosphorus threshold [16–18] that limits algal growth with the aim of regulating algal proliferation and preventing the occurrence of algal blooms.

Reports showed that the dominant algal species in algal blooms in major lakes in China [19–22] are primarily members of Cyanobacteria and Chlorophyta. Among these species, *Microcystis aeruginosa* and *Chlorella* are the most prevalent. In consideration of the representative algal species in Chinese lake ecosystems and laboratory conditions, this study selected *M. aeruginosa*, *Microcystis wesenbergii*, and *Chlorella vulgaris* as research subjects. These three algal species exhibit distinctive biological characteristics. *M. aeruginosa*, a cyanobacterium with a spherical to ellipsoidal shape, belongs to the genus *Microcystis*, possesses robust nitrogen-fixing capabilities and resilience to eutrophic conditions; however, its bloom formation may produce microcystins, thus posing potential threats to ecosystems and human health. *M. wesenbergii*, also a cyanobacterium and belonging to the *Microcystis*, typically forms blooms in nutrient-rich waters and may produce toxins. *C. vulgaris*, a green alga belongs to the genus *Chlorella*, is known for its rapid growth and adaptability, often serving as a model organism in environmental and ecological research. While these algae play crucial roles in aquatic environments, their excessive proliferation can disrupt ecological balance and contribute to water quality issues. Therefore, exploring a method for controlling the excessive proliferation of algae to prevent the occurrence of algal blooms is necessary.

Although numerous studies have been conducted on the threshold of algal growth, their final conclusions do not elucidate the relationship between the growth-to-growth rate ratio of algae and thresholds. Furthermore, their threshold results vary considerably, making determining the precise numerical value that restricts algal growth challenging. For example, the conclusion derived by Xu et al. [23] in an in situ cultivation experiment on summer cyanobacterial blooms in Lake Taihu suggested an upper threshold for algal growth that is not limited by nutrients, with TP ranging from 0.15 mg/mL to 0.20 mg/L. Wu et al. [24], by using the frequency distribution method, estimated that the lower TP threshold value limiting algal growth is 0.059 mg/L, which is comparable to the findings of our study. Additionally, several studies have discussed TP thresholds for maintaining water bodies in a sub-bloom state. For example, the in situ cultivation experiments [25] conducted by Xu et al. on Lake Taihu and Meiliang Bay [26] suggested that maintaining TP concentrations below 0.08 mg/L is effective for controlling the frequency and intensity of harmful algal blooms. The OECD [27], on the basis of expert opinions, considers the TP threshold for eutrophication in water bodies to be 0.084 mg/L. Gibson et al. [28] proposed that the occurrence of cyanobacterial blooms becomes possible when TP concentrations exceed 0.01 mg/L.

As can be observed from the above studies, numerous conclusions regarding the threshold of algae exists, but a consensus on which concentration can effectively restrict algal growth has not been reached. In response to this uncertainty, we formulated a scientific hypothesis based on the Monod equation [29]. We propose that a significant correlation exists between the growth-to-growth rate ratio of algae and the phosphorus threshold. We posit the existence of a specific phosphorus concentration, denoted as S' , at which the growth-to-growth rate ratio of algae reaches zero. When the growth-to-growth rate ratio is zero, algal outbreaks are effectively controlled. We introduce an improved Monod equation and design experiments for verification to validate our hypothesis. Our conclusive experimental results confirm the feasibility of our hypothesis.

1.1. Monod Equation

In 1949, Monod published a study that systematically examined results from static reactors, associating cell-specific growth rates with the limiting substrate concentration in a functional manner [29]. He suggested that the relationship between microbial specific growth rate and substrate concentration could be described using the classical Michaelis–Menten equation, leading to the development of the Monod equation:

$$\frac{1}{X} \frac{dX}{dt} = \mu = \mu_{\max} \frac{S}{K_s + S} \quad (1)$$

In this context, μ_{\max} represents the maximum specific growth rate of microorganisms, and K_s stands for the saturation constant, which corresponds to the substrate concentration when μ equals half of μ_{\max} . It is also known as the half-velocity constant. S represents the concentration of organic substrate, and X is the concentration of microorganisms. The curve of the Monod equation is depicted in Figure 1 [30]. The Monod equation, in its empirical form, is widely utilized in contemporary wastewater biological treatment as a powerful tool to guide indicators, such as organic load, in biological treatment.

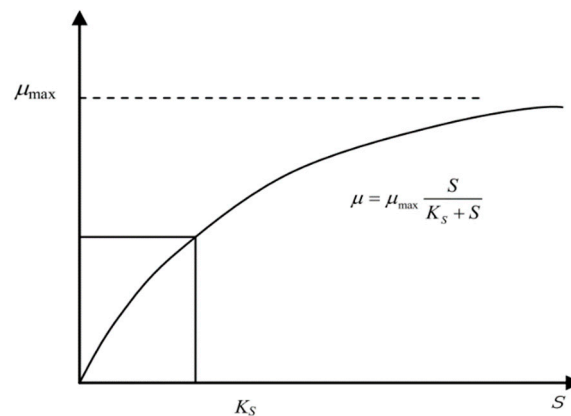


Figure 1. Monod equation and its $\mu = f(S)$ curve.

1.2. Modified Monod Model

The Monod equation, as one of the most widely used mathematical models in microbial growth studies, holds considerable theoretical and practical importance. However, it still exhibits certain limitations. As observed in Figure 1, the Monod equation represents a curve starting from the point (0, 0), indicating that when the substrate concentration S is zero, the specific growth rate of microorganisms is also zero. As noted in related studies [31], the Monod equation provides the relationship between the specific growth rate of fast-growing bacteria and the electron donor concentration that limits their growth:

$$\mu_{syn} = \left(\frac{1}{X_a} \frac{dX_a}{dt} \right)_{syn} = \hat{\mu} \frac{S}{K + S} \quad (2)$$

Here, μ_{syn} represents the synthesized specific growth rate, X_a is the concentration of active bacterial cells (MxL^{-3}), t is time (T), S is the substrate concentration limiting the growth rate (MSL^{-3}), $\hat{\mu}$ is the maximum specific growth rate (T^{-1}), and K is the substrate concentration at which the growth rate is half of the maximum specific growth rate (MSL^{-3}). Figure 2 illustrates the variation in μ with S and the condition where $\mu = \hat{\mu}/2$ when $K = S$.

Researchers focusing on slowly growing bacteria, such as environmental engineers, have observed that active bacterial cells require energy to sustain their life activities, including movement, repair and synthesis, osmoregulation, transport, and heat dissipation, among other cellular functions. Environmental engineers often use the term “endogenous decay” to describe the energy and electron flow required to sustain growth. In other words, cells oxidize themselves to meet the energy requirements necessary for maintenance.

The rate of endogenous decay is determined by the following equation:

$$\mu_{dec} = \left(\frac{1}{X_a} \frac{dX_a}{dt} \right)_{decay} = -b. \tag{3}$$

In the above equation, b represents the endogenous decay coefficient (T^{-1}), and μ_{dec} denotes the specific growth rate considering decay (T^{-1}).

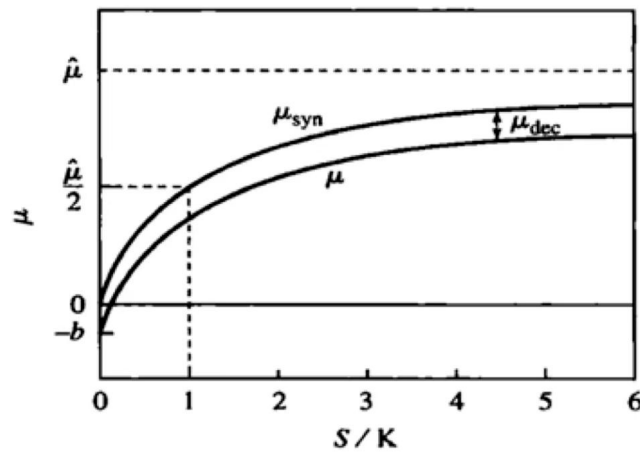


Figure 2. Schematic of synthesis and net growth rates as a function of substrate concentration.

Equation (3) illustrates that the loss of active bacterial cells can be described by using a first-order function. However, in reality, not all lost active bacterial cells undergo oxidation to generate the energy required for microbial maintenance. Although the majority of decaying cells undergo oxidation, a small fraction accumulates in the form of inert cells. The oxidation rate (respiration, which is the process that is truly utilized to generate energy) is determined by

$$\left(\frac{1}{X_a} \frac{dX_a}{dt} \right)_{resp} = -f_d b. \tag{4}$$

In the above equation, f_d represents the fraction of biodegradable compounds within active bacterial cells. The rate at which active bacterial cells transform into inert cells is determined by the difference between the overall decay rate and the oxidation rate:

$$-\frac{1}{X_a} \frac{dX_i}{dt} = \left(\frac{1}{X_a} \frac{dX_a}{dt} \right)_{inert} = -(1 - f_d)b \tag{5}$$

In the above equation, X_i represents the concentration of inert bacterial cells (MxL^{-3}). Overall, the net specific growth rate (μ) of active bacterial cells is the sum of new growth (Equation (2)) and decay (Equation (3)):

$$\mu = \frac{1}{X_a} \frac{dX_a}{dt} = \mu_{syn} + \mu_{dec} = \hat{\mu} \frac{S}{K + S} - b \tag{6}$$

Figure 2 also illustrates the variation in μ with S , indicating that under sufficiently low S conditions, μ may be negative.

The specific growth rate μ of algae can also be negative. In terms of the effect of phosphorus on algal cell growth, phosphorus is an essential component of algal cell phospholipids, nucleic acids, and other important substances. It directly influences the storage and transfer of energy and information within active cells, making it a crucial factor in algal cell growth. Research indicates the occurrence of luxury phosphorus uptake [32,33] in the absorption of phosphorus by algae. The phosphorus absorbed during this process is stored intracellularly in the form of polyphosphate bodies. These internal phosphorus [34–36]

reserves emerge as critical factors influencing cell division [37,38]. Excessive reductions in phosphorus concentrations not only affect the absorption of other elements, such as nitrogen [39], by cells but also hinders the ability of cells to undergo photosynthesis [40], ultimately suppressing cell growth [41]. Therefore, in low-phosphorus concentration culture media, some cells may die due to lysis, and overall, the cell proliferation rate is lower than the decay rate, resulting in a negative net growth rate.

In this work, we attempt to apply the theory developed above to the study of algal growth and propose a modified Monod model that describes the relationship between the specific growth rate of algae and the limiting concentration of phosphorus nutrients:

$$\frac{1}{X} \frac{dX}{dt} = \mu = \mu_{max} \frac{S}{K_s + S} + C. \quad (7)$$

In the above equation, μ represents the specific growth rate of algae, expressed in day^{-1} ; S denotes the concentration of the limiting substrate phosphorus, measured in mg/L ; t stands for time, measured in days; X represents algal density; μ_{max} corresponds to the maximum specific growth rate, expressed in day^{-1} ; K_s is the phosphorus concentration at which algal growth reaches half of the maximum specific growth rate, measured in mg/L ; and C represents the specific death rate of algal growth, expressed in day^{-1} .

Setting Equation (7) to zero yields:

$$S' = \frac{K_s \mu_{max} C}{1 - \mu_{max} C}. \quad (8)$$

The term S' is defined as the lower threshold concentration of phosphorus at which the algal specific growth rate becomes zero. Its importance lies in the fact that when phosphorus becomes the limiting factor for algal growth, thus maintaining the phosphorus concentration at the level of S' , the specific growth rate of algae equals their specific death rate. At this point, algal growth reaches a dynamic equilibrium state. This situation has practical implications for controlling algal blooms.

2. Materials and Methods

Cultivation experiments were designed for algae under various phosphorus concentrations to validate the proposed modified Monod model described above. The nonlinear curve fitting analysis of the specific growth rate μ of algae against phosphorus concentration was conducted to assess the correlation between algal growth patterns under phosphorus limitation and the modified model.

2.1. Experimental Materials

The original algal strains used in this experiment were obtained from the Freshwater Algae Culture Collection of the Chinese Academy of Sciences. They included *M. aeruginosa* (FACHB-315), *C. vulgaris* (FACHB-8), and *M. wesenbergii* (FACHB-908). Other experimental materials are detailed in the Appendix A.

2.2. Medium Design

Three types of media were used in the experiments: initial culture medium, phosphate-deficient medium, and phosphate concentration gradient medium. The initial culture medium was prepared by using BG11 medium. The phosphate-deficient medium was derived from BG11 medium by excluding a phosphate source (K_2HPO_4). The specific formulations for the three types of culture media are provided in the Appendix A.

2.3. Experimental Design

All experimental operations were conducted under aseptic conditions. First, algae were subjected to nutrient deprivation in a phosphorus-free culture medium. Subsequently, they were inoculated into a culture medium with a phosphorus concentration gradient and

placed in an experimental incubator. Sampling was conducted at 24 h intervals to measure the algal density of each species. Refer to the Appendix A for detailed experimental procedures and conditions.

2.4. Data Analysis Methods

The raw data obtained after 7 days of experimentation included the daily algal density X at various concentrations of the culture medium along with the time interval t between each sampling. The formula used to calculate the algal specific growth rate is as follows:

$$\mu = \frac{1}{X} \frac{dX}{dt}. \quad (9)$$

By integrating both sides of the equation, we obtain

$$\mu t = \ln(X) + C. \quad (10)$$

By compiling results, we obtain

$$\ln X = \mu t - C. \quad (11)$$

By utilizing the Matlab(R2022a) processing tool, we performed linear regression on the natural logarithm of algal density values ($\ln[X]$) against the time interval t , obtaining the slope of this equation as the specific growth rate μ of the algae at different concentrations.

Furthermore, we employed the AR toolbox within Matlab to conduct nonlinear regression on the relationship between the algal specific growth rate μ and phosphorus concentration, as per Equation (7), to investigate the accuracy of the modified Monod equation.

3. Results and Analysis

The experiment involved fitting data for each algal species twice to minimize random errors during data processing. The linear regression of algal specific growth rate was performed by using the logarithm of the average of 15 algal density values (\bar{X}) obtained from three parallel samples at each phosphorus concentration. Additionally, the logarithm of the average algal density values ($\bar{X}_1, \bar{X}_2, \bar{X}_3$) for each set of parallel samples at each phosphorus concentration was calculated, and linear regression analysis was conducted against the cultivation time t .

3.1. Specific Growth Rate of *C. vulgaris*

The fitting plot of $\ln(\bar{X})$ for *C. vulgaris* against time t is shown in Figures 3–10, and the fitting results are presented in Table 1.

The fitted curve of the $\ln(\bar{X}_1, \bar{X}_2, \bar{X}_3)$ values of *C. vulgaris* with respect to time are shown in Figures 11–18, and the fitting results are presented in Table 2.

As can be observed in Figures 3–18, a clear linear relationship exists between the $\ln(X)$ values of *C. vulgaris* and time t . In accordance with Equation (11), the slope of the fitted linear equation represents the specific growth rate of *C. vulgaris*. Combining the results in Tables 1 and 2 show that the fitting results from both sets of data are close and that the R^2 values of the fitting are generally high, indicating a significant linear relationship between the two variables. This situation suggests the validity of the results.

C. vulgaris growth exhibits a certain degree of inhibition at low phosphorus concentrations (Tables 1 and 2) because the specific growth rates are negative. However, no significant cell death occurs, and algal cells experience a slow rate of decline. As phosphorus concentration increases, the specific growth rate of *C. vulgaris* approaches zero, indicating a dynamic equilibrium between growth and decline, whereas the algal cell population remains relatively constant. When the phosphorus concentration exceeds 0.07 mg/L, the growth and reproduction of *C. vulgaris* improve with increasing initial phosphorus concentrations, and thus algal biomass increases. When the phosphorus concentration reaches 1.06–2.13 mg/L, the variation in the specific growth rate of *C. vulgaris* is not significant. This result indicates

that the concentration has approached the saturation point for phosphorus absorption by *C. vulgaris*, representing the upper threshold limit at which phosphorus concentration affects the growth of *C. vulgaris*. This result is consistent with the findings of Sun et al. [42].

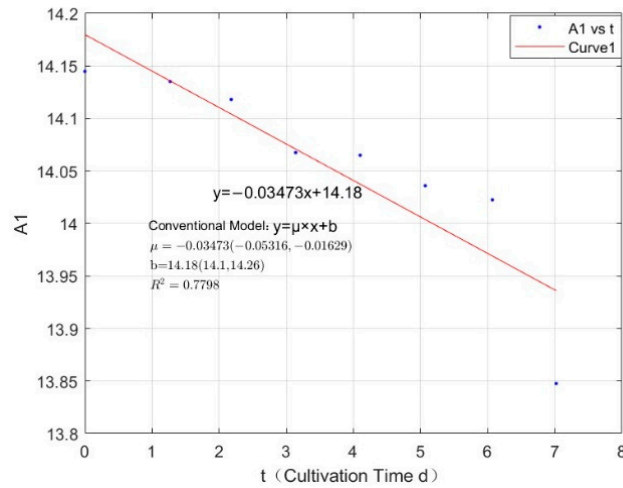


Figure 3. Fitted plot for *C. vulgaris* at Concentration A1.

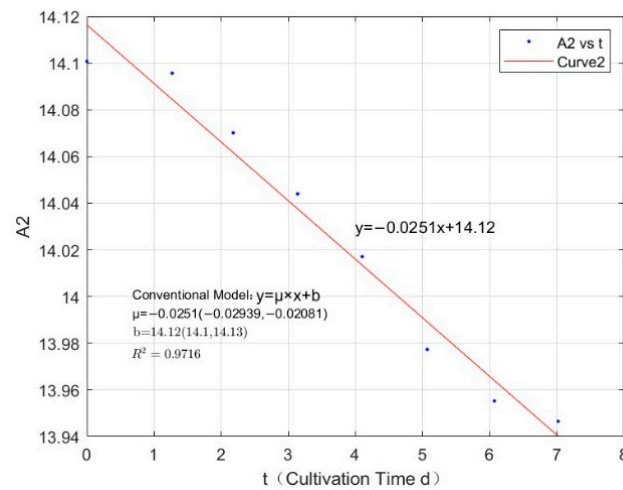


Figure 4. Fitted plot for *C. vulgaris* at Concentration A2.

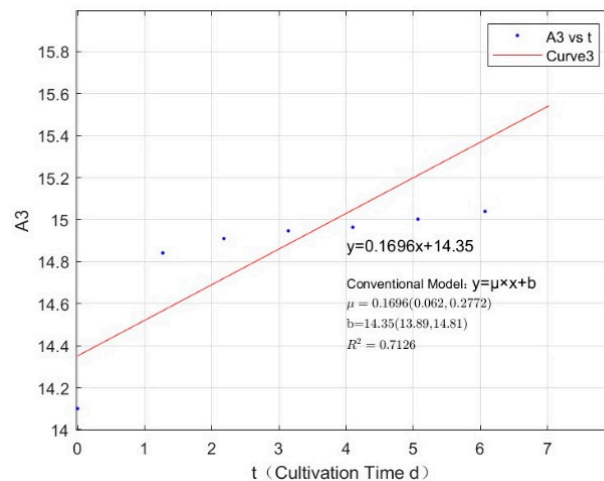


Figure 5. Fitted plot for *C. vulgaris* at Concentration A3.

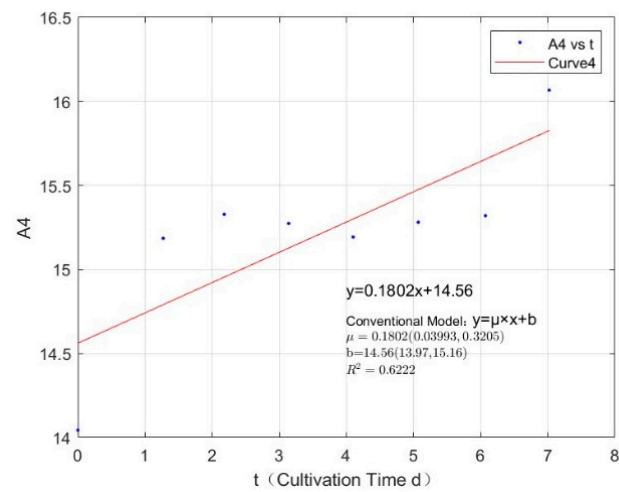


Figure 6. Fitted plot for *C. vulgaris* at Concentration A4.

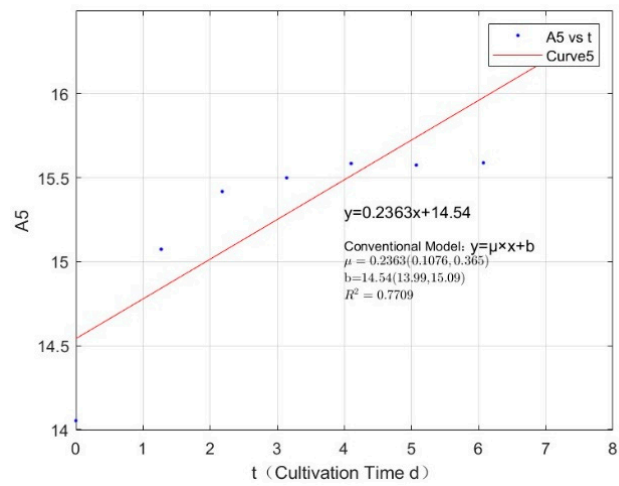


Figure 7. Fitted plot for *C. vulgaris* at Concentration A5.

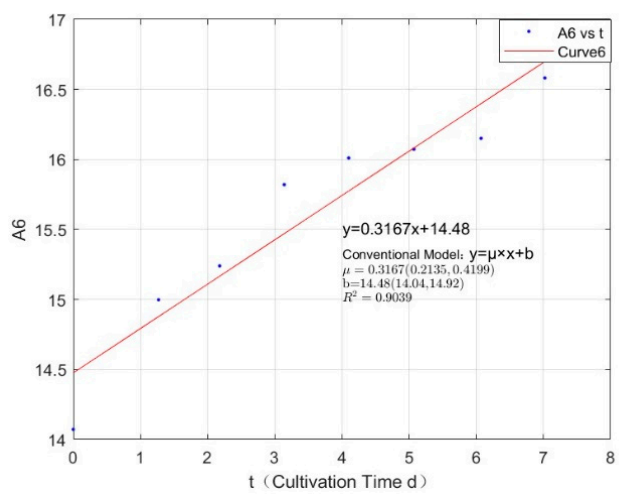


Figure 8. Fitted plot for *C. vulgaris* at at Concentration A6.

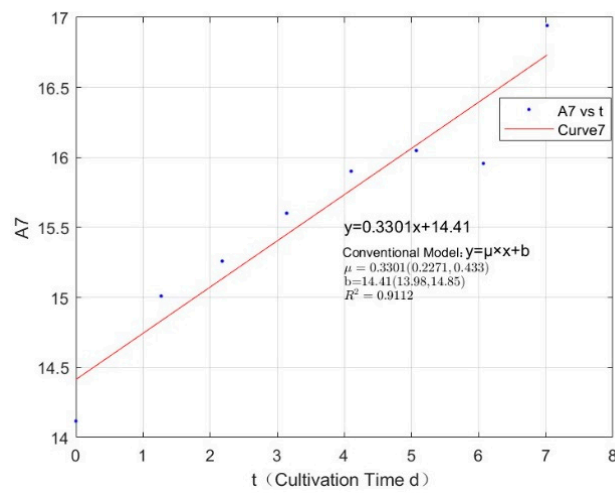


Figure 9. Fitted plot for *C. vulgaris* at Concentration A7.

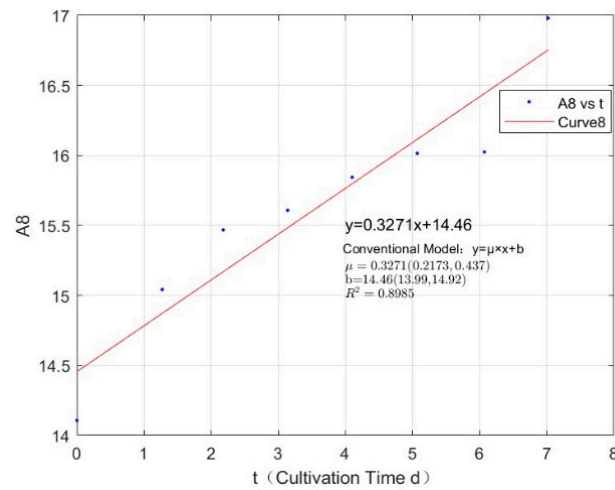


Figure 10. Fitted plot for *C. vulgaris* at Concentration A8.

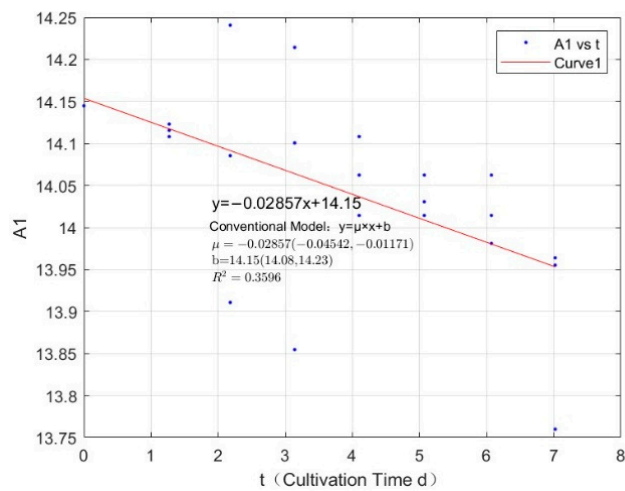


Figure 11. Fitted plot for *C. vulgaris* at Concentration A1.

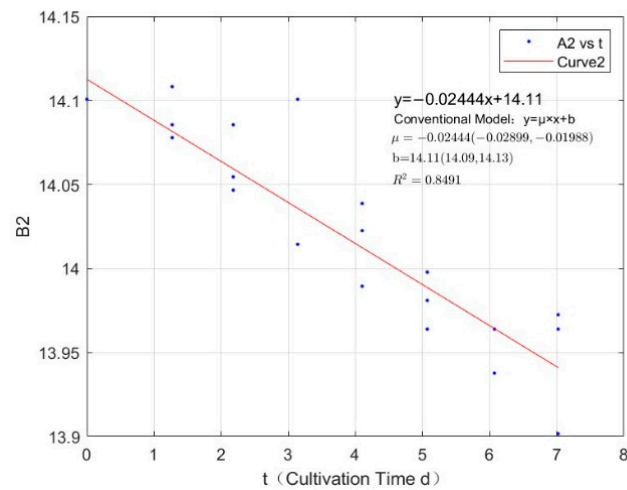


Figure 12. Fitted plot for *C. vulgaris* at Concentration A2.

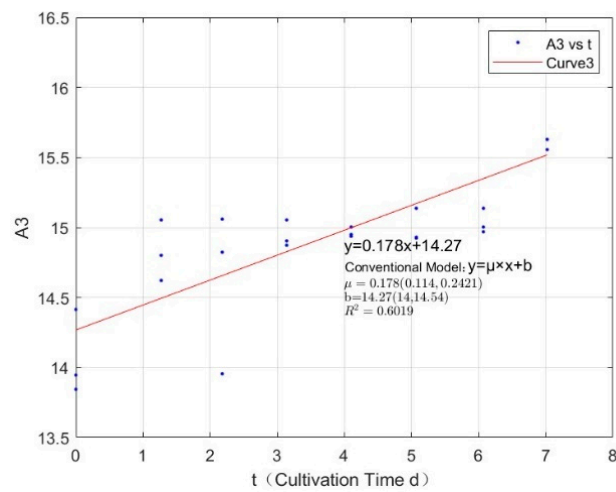


Figure 13. Fitted plot for *C. vulgaris* at Concentration A3.

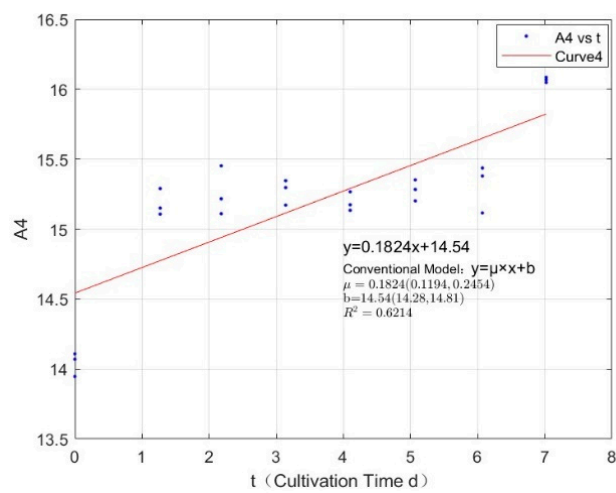


Figure 14. Fitted plot for *C. vulgaris* at Concentration A4.

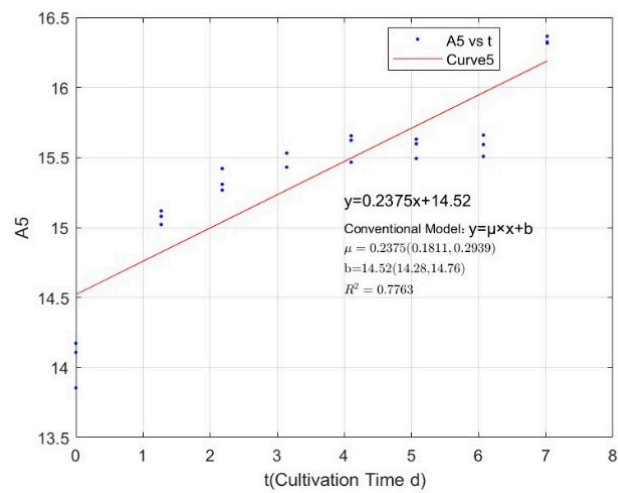


Figure 15. Fitted plot for *C. vulgaris* at Concentration A5.

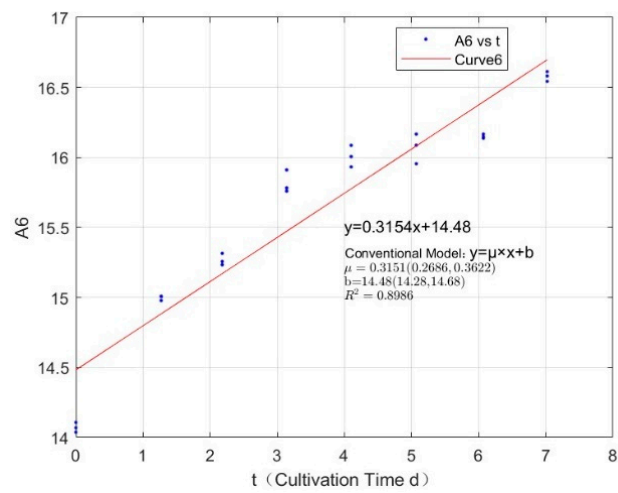


Figure 16. Fitted plot for *C. vulgaris* at Concentration A6.

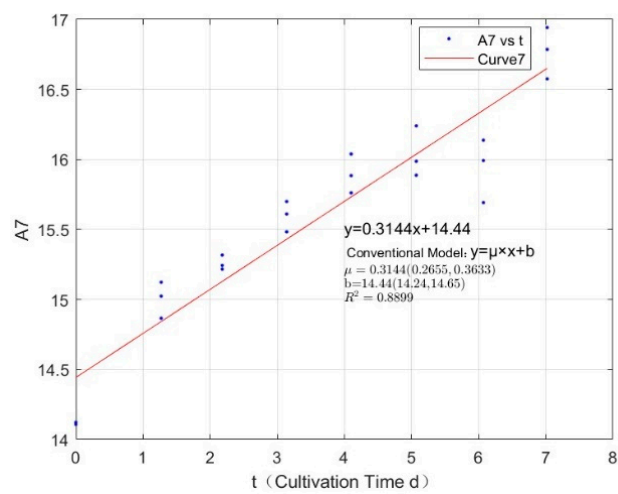


Figure 17. Fitted plot for *C. vulgaris* at Concentration A7.

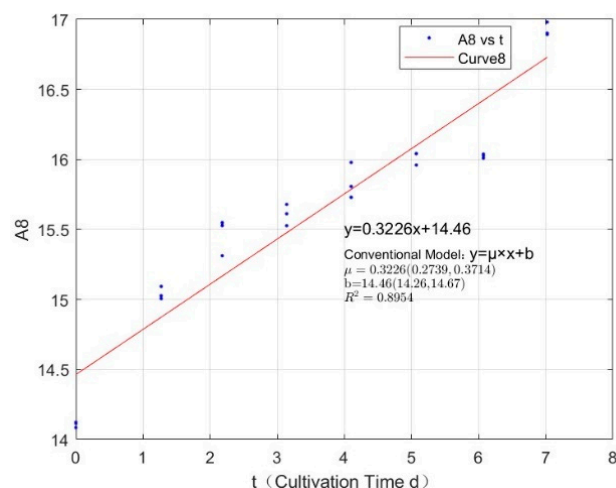


Figure 18. Fitted plot for *C. vulgaris* at Concentration A8.

Table 1. Specific growth rate of *C. vulgaris* at different phosphorus concentrations.

Phosphorus Concentration (mg/L)	Specific Growth Rate (day ⁻¹)	Fitted R-Squared Value (R ²)
0.0356	−0.0347	0.7798
0.0711	−0.0251	0.9716
0.1423	0.1696	0.7126
0.2134	0.1802	0.6222
0.3557	0.2363	0.7709
1.0671	0.3167	0.9039
2.1342	0.3301	0.9112
2.7745	0.3271	0.8985

Table 2. Specific growth rate of *C. vulgaris* at different phosphorus concentrations.

Phosphorus Concentration (mg/L)	Specific Growth Rate (day ⁻¹)	Fitted R-Squared Value (R ²)
0.0356	−0.0286	0.3596
0.0711	−0.0244	0.8491
0.1423	0.178	0.6019
0.2134	0.1824	0.6214
0.3557	0.2375	0.7763
1.0671	0.3154	0.8986
2.1342	0.3144	0.8899
2.7745	0.3226	0.8954

3.2. Growth Rate of *M. aeruginosa*

The fitting plots of $\ln(\bar{X})$ for *M. aeruginosa* in relation to time (t) are presented in Appendix B, Figures A1–A8, and the fitting results are shown in Table 3.

The fitted curves of $\ln(\bar{X}_1, \bar{X}_2, \bar{X}_3)$ values of *M. aeruginosa* in relation to time are shown in Appendix B, Figures A9–A16, and the fitting results are presented in Table 4.

The natural logarithm of *M. aeruginosa* ($\ln[X]$) values show a clear linear relationship with time (t) (Appendix B, Figures A1–A16), indicating a good fit of the data. When the phosphorus concentration is 0.0356 mg/L, the growth of *M. aeruginosa* is somewhat inhibited (Tables 3 and 4). However, when the phosphorus concentration reaches 0.0711 mg/L, *M. aeruginosa* exhibits rapid growth and reproduction. The lower limit threshold at which phosphorus limits the growth of *M. aeruginosa* falls between 0.0356 and 0.0711 mg/L. Furthermore, once phosphorus concentration exceeds this lower threshold, the proliferation rate of *M. aeruginosa* significantly increases. This rate continues to increase with phosphorus

concentration, reaching a maximum value of 2.1342 mg/L. Beyond this point, the specific growth rate of *M. aeruginosa* slightly decreases, indicating that excessively high phosphorus levels may have a mild inhibitory effect on its growth.

Table 3. Specific growth rate of *M. aeruginosa* at different phosphorus concentrations.

Phosphorus Concentration (mg/L)	Specific Growth Rate (day ⁻¹)	Fitted R-Squared Value (R ²)
0.0356	−0.0397	0.9486
0.0711	0.2308	0.9238
0.1423	0.3048	0.9411
0.2134	0.3562	0.9434
0.3557	0.4339	0.9675
1.0671	0.4863	0.9846
2.1342	0.5108	0.9773
2.7745	0.4842	0.9873

Table 4. Specific growth rate of *M. aeruginosa* at different phosphorus concentrations.

Phosphorus Concentration (mg/L)	Specific Growth Rate (day ⁻¹)	Fitted R-Squared Value (R ²)
0.0356	−0.0369	0.7486
0.0711	0.2317	0.8806
0.1423	0.3047	0.9338
0.2134	0.3564	0.9386
0.3557	0.4339	0.9613
1.0671	0.4873	0.9793
2.1342	0.5065	0.9783
2.7745	0.4876	0.9815

3.3. Growth Rate of *M. wesenbergii*

The fitting plots of $\ln(\bar{X})$ for *M. wesenbergii* in relation to time (t) are presented in Appendix B, Figures A17–A24, and the fitting results are shown in Table 5.

Table 5. Specific growth rate of *M. wesenbergii* at different phosphorus concentrations.

Phosphorus Concentration (mg/L)	Specific Growth Rate (day ⁻¹)	Fitted R-Squared Value (R ²)
0.0356	0.0955	0.3495
0.0711	0.1891	0.8780
0.1423	0.2416	0.9411
0.2134	0.2907	0.9814
0.3557	0.3231	0.9864
1.0671	0.3099	0.9765
2.1342	0.3535	0.9946
2.7745	0.3123	0.9907

The fitted curves of the $\ln(\bar{X}_1, \bar{X}_2, \bar{X}_3)$ values of *M. wesenbergii* with time are shown in Appendix B, Figures A25–A32, and the fitting results are presented in Table 6.

The natural logarithm values of *M. wesenbergii* exhibit a clear linear relationship with time (t) (Appendix B Figures A17–A32), indicating favorable fitting results. When the phosphorus concentration is relatively low (0.0356 mg/L), *M. wesenbergii* exhibits minimal growth rates (Tables 5 and 6). However, the specific growth rate of *M. wesenbergii* gradually increases with phosphorus concentration (0.0711–0.3557 mg/L), suggesting that the limiting phosphorus nutrient threshold for the growth of *M. wesenbergii* is likely below 0.0356 mg/L. Mathematical modeling can be used to calculate the theoretical lower threshold that restricts its growth.

Table 6. Specific growth rate of *M. wesenbergii* at different phosphorus concentrations.

Phosphorus Concentration (mg/L)	Specific Growth Rate (day ⁻¹)	Fit R-Squared Value (R ²)
0.0356	0.1019	0.4399
0.0711	0.1926	0.8860
0.1423	0.2455	0.9493
0.2134	0.2868	0.9843
0.3557	0.3259	0.9890
1.0671	0.3136	0.9722
2.1342	0.3621	0.9929
2.7745	0.3177	0.9846

When the phosphorus concentration exceeds this lower threshold, the proliferation rate of *M. wesenbergii* considerably increases, continues to increase until a phosphorus concentration of 2.1342 mg/L, and then decreases. Thus, excessively high phosphorus nutrient levels may exert inhibitory effects on the growth of *M. wesenbergii*.

4. Comparison and Discussion Based on the Experiment of Specific Growth Rate of Three Kinds of Algae

4.1. Comparison of the Specific Growth Rates of Three Algal Species

The comparative line chart depicting the specific growth rates of *C. vulgaris*, *M. aeruginosa*, and *M. wesenbergii* is presented in Figure 19.

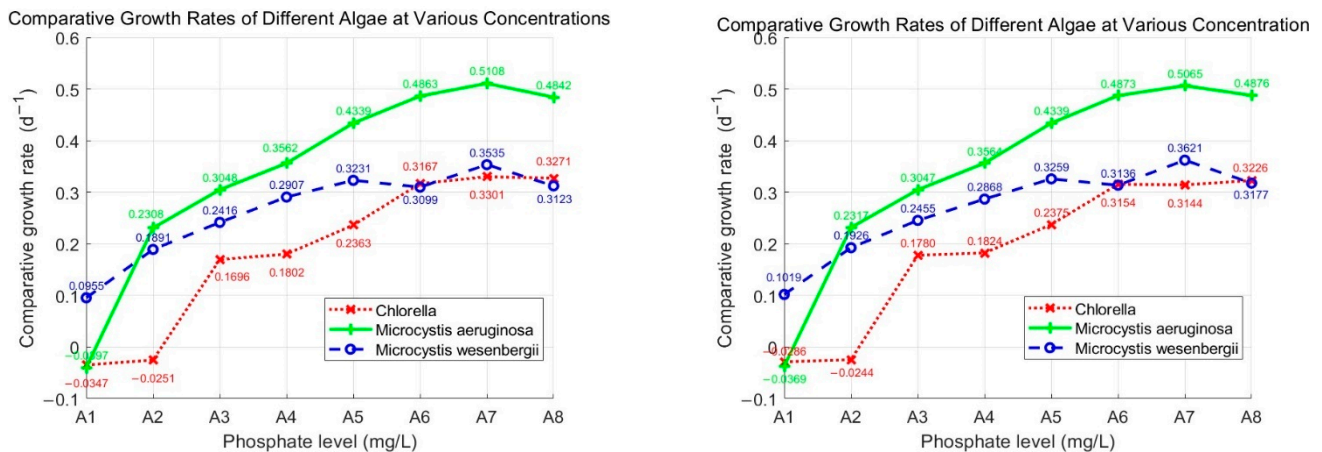


Figure 19. Comparison of algal specific growth rates.

Variations in the specific growth rates of *C. vulgaris*, *M. aeruginosa*, and *M. wesenbergii* exhibit similar trends at the same phosphorus concentrations (Figure 19). This is characterized by inhibited or reduced growth at low phosphorus concentrations, followed by an increase in specific growth rates as phosphorus concentration increases. However, as phosphorus concentration exceeds a certain threshold, the rate of increase in specific growth rates decreases.

In the comparative graph, *M. aeruginosa* and *C. vulgaris* have similar specific growth rates at a low phosphorus concentration (A1 0.0356 mg/L), whereas *M. wesenbergii* shows positive growth but with an extremely low specific growth rate. When the phosphorus concentration reaches the A2 concentration (0.0711 mg/L), *C. vulgaris* growth is still inhibited, and the specific growth rates of *M. aeruginosa* and *M. wesenbergii* exhibit a geometrically increasing trend, which suggests that the phosphorus nutrient thresholds of *M. aeruginosa* and *M. wesenbergii* are lower than the phosphorus nutrient threshold of *C. vulgaris*. *M. aeruginosa* has a higher specific growth rate than *C. vulgaris* and *M. wesenbergii* at various phosphorus nutrient concentrations. Thus, *M. aeruginosa* is more likely to gain a competitive advantage and become the dominant species, possibly explaining the prevalence of

cyanobacterial blooms in China. When the phosphorus concentration is at the A5 concentration (0.3557 mg/L), the specific growth rates of *C. vulgaris* and *M. wesenbergii* nearly reach maximum values. Subsequent increases in phosphorus concentration have minimal effects on these two algal species, indicating that the upper threshold for their growth lies at approximately 0.3557 mg/L. This results aligns with existing research conclusions. By contrast, the specific growth rate of *M. aeruginosa* continues to increase with phosphorus concentration. At high phosphorus concentrations (>A7), *C. vulgaris* is essentially in a stable growth state and is almost unaffected by phosphorus concentration. The specific growth rate of *M. aeruginosa* slightly decreases, whereas that of *M. wesenbergii* shows a considerable decrease. This result suggests that the inhibitory effect of high phosphorus concentrations may not apply to all algal species and phosphorus concentration considerably affects the growth of *M. aeruginosa* and *M. wesenbergii*.

4.2. Fitting of the Modified Monod Model for *C. vulgaris*

The nonlinear fitting of the specific growth rates of *C. vulgaris* against phosphorus nutrient concentration follows Equation (7) and is illustrated in Figure 20.

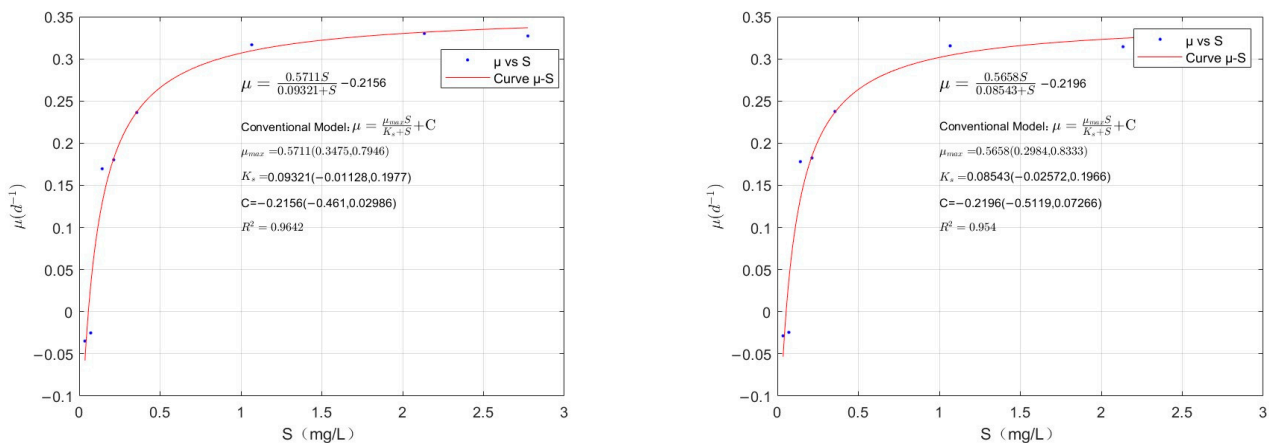


Figure 20. Modified Monod model fitting for *C. vulgaris*.

The conventional model used for fitting is the modified Monod equation (Equation (7)): $\mu = \mu_{max} \frac{S}{K_s + S} - C$. The coefficients of the equation (with a 95% confidence interval) obtained from the fitting results are as follows: μ_{max} (0.5711, 0.5658), K_s (0.09321, 0.08543), and C (0.2156, 0.2196). The goodness-of-fit indicators include sum of squared errors (SSE) (0.005515, 0.006661), coefficient of determination (R^2) (0.964, 0.954), adjusted R^2 (0.9498, 0.9357), and root-mean-squared error (RMSE) (0.03321, 0.0365).

The R^2 values obtained from the fitting indicate that the proposed modified Monod equation effectively reflects the nonlinear relationship between *C. vulgaris* growth rate and phosphorus nutrient concentration, validating the feasibility of the research hypothesis. This equation can describe the growth of *C. vulgaris* subjected to limited phosphorus nutrient. Additionally, the threshold phosphorus nutrient concentrations limiting *C. vulgaris* growth are 0.057 and 0.054 mg/L according to Equation (8). Wu et al. [19] concluded that the threshold for algal growth is a total phosphorus content of 0.059 mg/L, which aligns well with the results of this experiment.

Therefore, the proposed model provides a specific method for calculating the phosphorus limitation threshold in controlling nutrient-deficient algae. By maintaining the phosphorus concentration in water at approximately 0.054 mg/L, the growth of *C. vulgaris* can be maintained in a dynamic equilibrium state, and the excessive proliferation and the outbreak of algal blooms in aquatic ecosystems can thereby be effectively prevented.

4.3. Fitting of the Modified Monod Model for *M. aeruginosa*

The growth rate of *M. aeruginosa* in relation to phosphorus nutrient concentration was fitted by using Equation (7). The fitting graph is presented in Figure 21.

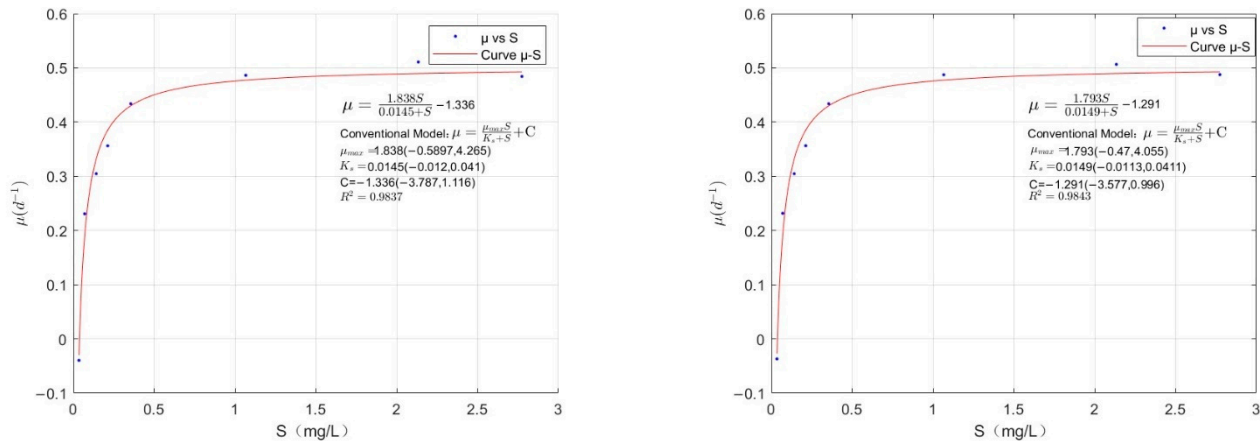


Figure 21. Modified Monod model fitting for *M. aeruginosa*.

The conventional model used for fitting is the modified Monod equation presented in Equation (7): $\mu = \mu_{\max} \frac{S}{K_s + S} - C$. The coefficients obtained from the fitting results (with 95% confidence intervals) are as follows: μ_{\max} (1.838, 1.793), K_s (0.0145, 0.0149), and C (1.336, 1.291). The goodness-of-fit indicators include SSE (0.003874, 0.003697), R^2 (0.9837, 0.9843), adjusted R^2 (0.977, 0.978), and RMSE (0.02784, 0.02719).

The obtained R^2 values from the fitting indicate that the modified Monod equation proposed in this study (Equation (7)) effectively represents the nonlinear relationship between *M. aeruginosa* growth rate and phosphorus nutrient concentration. This validates the feasibility of the research hypothesis. The modified Monod model can describe the growth of *M. aeruginosa* under phosphorus nutrient limitation. Furthermore, the calculated phosphorus nutrient lower threshold for limiting the growth of *M. aeruginosa* is 0.039 mg/L (or 0.038 mg/L). This result provides a specific reference for nutrient control under oligotrophic conditions, implying that controlling phosphorus concentration in water at approximately 0.038 mg/L can help maintain a dynamic equilibrium in *M. aeruginosa* growth and thereby prevent the excessive proliferation of algae and occurrence of algal blooms.

4.4. Fitting of the Modified Monod Model for *M. wesenbergii*

The growth rate of *M. wesenbergii* was fitted against phosphorus nutrient concentration by using Equation (7) through nonlinear fitting. The fitting results are illustrated in Figure 22.

The conventional model used for fitting is the modified Monod equation as previously introduced in Equation (7): $\mu = \mu_{\max} \frac{S}{K_s + S} - C$. The fitting results yielded the coefficients (with 95% confidence intervals) of μ_{\max} : (0.7112, 0.6112); K_s : (0.0186, 0.0234); and C : (0.3732, 0.2675). The goodness-of-fit metrics included SSE: (0.001879, 0.001902); R^2 : (0.9633, 0.9626); adjusted R^2 : (0.9486, 0.9477); and RMSE: (0.01939, 0.0195).

The R^2 values obtained from the fitting indicate that the modified Monod equation (Equation (7)) proposed in this study effectively reflects the nonlinear relationship between the growth rate of *M. wesenbergii* and concentration of phosphorus nutrients, thus validating the feasibility of our research hypothesis. This modified Monod model can describe the growth of *M. wesenbergii* under phosphorus limitation. Furthermore, Equation (8) allows the calculation of the phosphorus lower threshold that restricts the growth of *M. wesenbergii*. The thresholds were approximately 0.039 and 0.038 mg/L. This study provides a specific phosphorus limitation threshold as a reference for controlling phosphorus concentration in water. Maintaining the phosphorus concentration in the range of approximately 0.038 mg/L

in water bodies potentially maintains the dynamic equilibrium of *M. wesenbergii* growth, thus preventing the excessive proliferation of algae and occurrence of algal blooms.

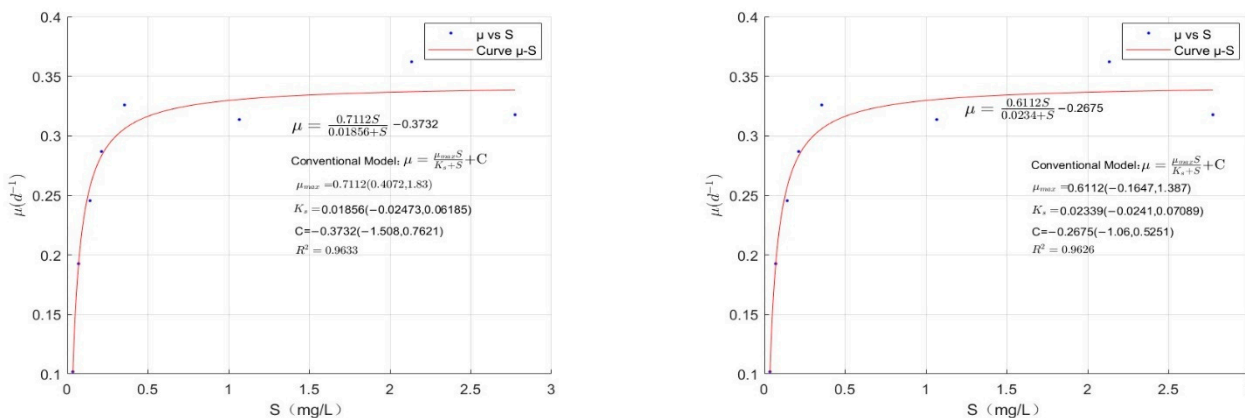


Figure 22. Modified Monod model fitting for *M. wesenbergii*.

4.5. Comparison of Modified Monod Models for *C. vulgaris*, *M. aeruginosa*, and *M. wesenbergii*

A comparative chart of the modified Monod models for *C. vulgaris*, *M. aeruginosa*, and *M. wesenbergii* is shown in Figure 23.

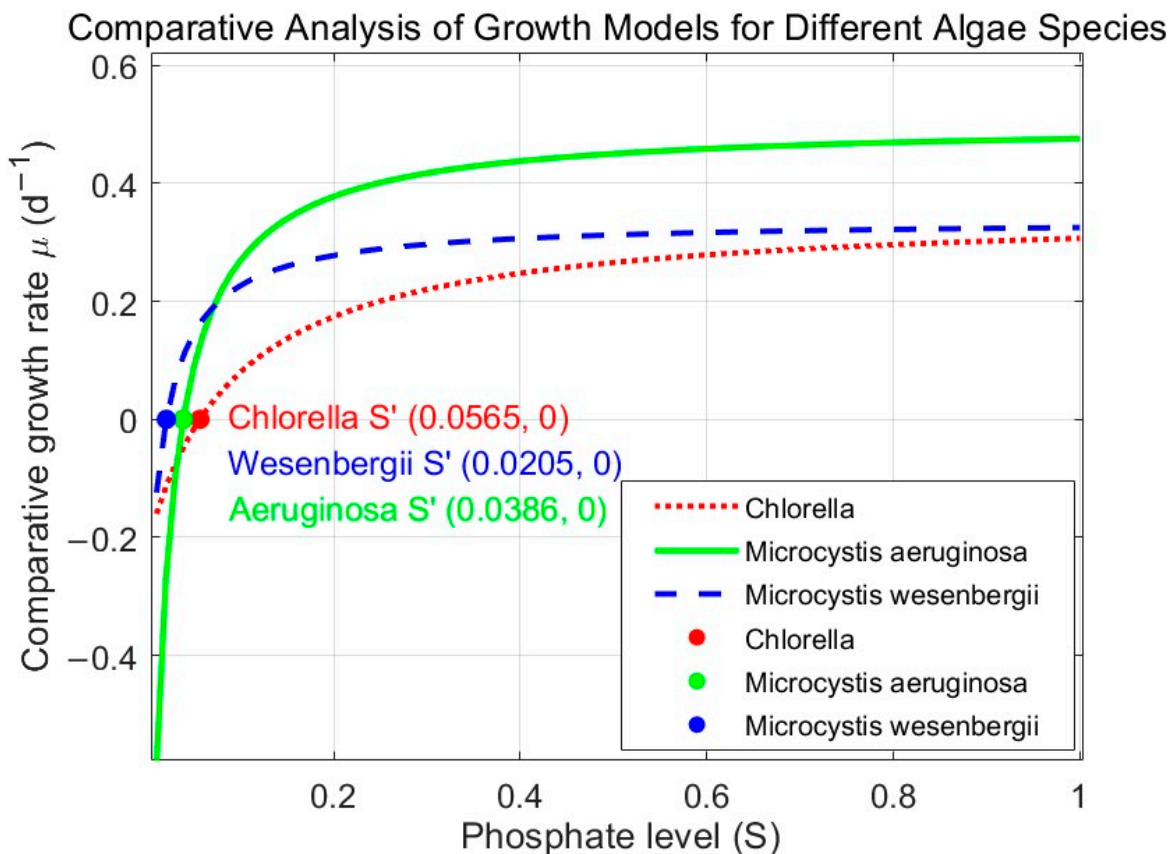


Figure 23. Comparison of modified Monod models for *C. vulgaris*, *M. aeruginosa*, and *M. wesenbergii*.

The coordinates of the equilibrium points (S') are (0.0565, 0), (0.0386, 0), and (0.0205, 0), and when phosphorus is limited, the corresponding phosphorus concentrations at which they maintain a growth rate of 0 are 0.0565, 0.0386, and 0.0205 mg/L. This concentration represents the phosphorus lower threshold for algal growth.

The phosphorus lower threshold for *M. wesenbergii* ($S' = 0.0205$ mg/L) is smaller than that for *M. aeruginosa* ($S' = 0.0386$ mg/L), and both thresholds are smaller than the

threshold for *C. vulgaris* ($S' = 0.0565$ mg/L). In other words, these thresholds follow the order of *M. wesenbergii* $S' < M. aeruginosa$ $S' < C. vulgaris$ S' . Furthermore, *M. wesenbergii* and *M. aeruginosa* show a greater increase in their growth rates than *C. vulgaris* at low phosphorus concentrations and increasing phosphorus nutrient levels. This result indicates that *M. wesenbergii* and *M. aeruginosa* require low phosphorus nutrient concentrations as a lower threshold for growth and exhibit fast growth rates at the same phosphorus concentration. Although *M. wesenbergii* has a lower phosphorus nutrient threshold than *M. aeruginosa*, the growth rate of *M. aeruginosa* is higher when phosphorus concentration further increases. The maximum growth rate of *M. aeruginosa* is considerably higher than that of *M. wesenbergii*. Thus, *M. aeruginosa* tends to become the dominant species. Therefore, algal blooms in Chinese lakes are primarily composed of cyanobacteria, and other algal species do not undergo blooms when cyanobacterial blooms occur.

5. Conclusions

In this study, phosphorus was considered as the controlled factor, and *C. vulgaris*, *M. aeruginosa*, and *M. wesenbergii* were selected as research subjects. While ensuring an excess supply of other nutrients, experiments were designed to investigate the relationship between algal growth and phosphorus concentration gradients. Additionally, a modified Monod model was established to determine the lower threshold of phosphorus nutrient concentration for the growth of different algal species. The following conclusions were drawn:

- (a) The conventional Monod equation has certain limitations. In this study, we proposed the modified Monod equation $\mu = \mu_{max} \frac{S}{K_s + S} + C$ and designed experiments to validate it. The resulting fit had R^2 values of 0.954, 0.964, 0.977, 0.978, 0.9633, and 0.9626, indicating that the modified Monod equation effectively describes algal growth when phosphorus is limited.
- (b) By using the modified Monod model, we calculated the lower threshold of phosphorus nutrients, which is the phosphorus nutrient concentration at which algal growth reaches a dynamic equilibrium. The calculated values were 0.0565 mg/L for *C. vulgaris*, 0.0386 mg/L for *M. aeruginosa*, and 0.0205 mg/L for *M. wesenbergii*. Controlling phosphorus concentrations at or near these S' values can theoretically prevent excessive algal proliferation, providing guidance for algal growth control using nutrient limitation.
- (c) The S' of the three algal species followed the order of *M. wesenbergii* $S' < M. aeruginosa$ $S' < C. vulgaris$ S' . *M. wesenbergii* requires the lowest theoretical phosphorus nutrient concentration for growth, followed by *M. aeruginosa*, and *C. vulgaris* requires the highest. The results suggest that cyanobacteria (*Microcystis* and similar species) have lower phosphorus nutrient thresholds, explaining why algal blooms in China are mainly composed of cyanobacteria and why other algal species do not bloom during cyanobacterial bloom events.
- (d) Among the three algal species, *M. aeruginosa* exhibited the highest maximum specific growth rate, whereas *C. vulgaris* had the lowest. This result suggests that in natural water bodies with fluctuating phosphorus concentrations, *M. aeruginosa* would dominate in terms of biomass, followed by *M. wesenbergii* and *C. vulgaris*. This observation implies that cyanobacterial biomass tends to be higher than that of green algae, making cyanobacteria the dominant species in freshwater ecosystems.
- (e) At high phosphorus concentrations (>2 mg/L), the growth of *M. aeruginosa* and *M. wesenbergii* is inhibited to some extent and that of *C. vulgaris* is unaffected. This result indicates that phosphorus inhibition does not occur in all algal species. The results of this experiment suggest that phosphorus inhibition is evident in cyanobacteria, and future research may explore this phenomenon further by investigating internal phosphorus forms and phosphorus absorption gene sequences in different algal species.

This study, combined with international and domestic research on algal growth under nitrogen and phosphorus thresholds, is in line with China's water quality conditions. It proposes the construction of a modified Monod model to describe algal growth, allowing the determination of the lower phosphorus nutrient threshold. The growth distribution trends of different algal species in freshwater ecosystems can be predicted and analyzed by comparing their lower thresholds. This information is crucial for controlling algal blooms through nutrient limitation. Moreover, this work constitutes a theoretical study based on laboratory conditions involving three algal species. Subsequent research can be extended to in situ experiments in lake environments. The experimental methods employed in this study are equally applicable to lake ecosystems; however, results may vary because of some factors, such as temperature variations and the influence of coexisting phytoplankton in lake water.

Author Contributions: Conceptualization, Y.G. and W.F.; methodology, Y.G.; software, Y.G.; validation, Y.G., W.F. and N.X.; formal analysis, Y.G.; investigation, Y.G.; resources, Y.G.; data curation, Y.G.; writing—original draft preparation, Y.G.; writing—review and editing, J.H. and Z.Z.; visualization, Y.G.; supervision, J.H.; project administration, J.H.; funding acquisition, J.H. All authors have read and agreed to the published version of the manuscript.

Funding: This research was funded by ABA Company grant number SCH1829202E and the APC was funded by Fudan University.

Data Availability Statement: The data presented in this study are available in the Appendices A and B of this article.

Acknowledgments: We would like to thank the ABA Company for providing financial support to this research.

Conflicts of Interest: The authors declare no conflict of interest.

Appendix A. Materials and Methods

Appendix A.1. Experimental Materials

Table A1. Experimental Materials.

Lab Equipment	Lab Equipment
BG11 medium (Changde Det Bio-Tech Co., Ltd.)	Photobioreactor
Centrifuge	Centrifuge tubes
Autoclave	Count Star cell counter
Count Star counting chamber	Analytical balance
1000 mL volumetric flasks	1000 mL volumetric flasks
500 mL Erlenmeyer flasks	Breathable membrane caps
Aseptic workbench	Alcohol lamp
Glass rods	Graduated cylinders
Wash bottles	Beakers
Pipettes	Wide-mouth bottles
Wide-mouth bottles (brown)	

Appendix A.2. Medium Design

Appendix A.2.1. Initial Culture Medium

The initial culture medium was prepared using BG11 medium. The specific recipe can be found in Table A2.

Table A2. BG11 Medium Recipe.

Drug Name	Dosage per Liter of Medium
NaNO ₃	1.5 g
K ₂ HPO ₄	0.04 g
MgSO ₄ ·7H ₂ O	0.075 g

Table A2. *Cont.*

Drug Name	Dosage per Liter of Medium
CaCl ₂ ·2H ₂ O	0.036 g
Citric acid	0.006 g
Ferric ammonium citrate	0.006 g
EDTANa ₂	0.001 g
Na ₂ CO ₃	0.02 g
A5	1 ml

Table A3. A5 formulation.

Drug Name	Usage per Liter of A5/mg
H ₃ BO ₃	2.86
MnCl ₂ ·4H ₂ O	1.86
ZnSO ₄ ·7H ₂ O	0.22
NaMoO ₄ ·2H ₂ O	0.021
CuSO ₄ ·5H ₂ O	0.08
Co(NO ₃) ₂ ·6H ₂ O	0.05

Appendix A.2.2. Phosphate-Deficient Medium

The phosphate-deficient medium was derived from BG11 medium by excluding the addition of a phosphate source (K₂HPO₄).

Appendix A.2.3. Phosphate Concentration Gradient Medium

The phosphate concentration gradient medium was prepared based on the BG11 medium by controlling the addition of potassium hydrogen phosphate (K₂HPO₄). The specific procedure is as follows: The standard BG11 medium consists of five stock solutions (Stock1...5), and their specific components are listed in Table A4. The concentration of phosphorus in the medium is determined by the amount of K₂HPO₄ added to Stock2 solution. Different concentrations of experimental Stock 2 solutions, denoted as a1, a2, a3...a8, were prepared using potassium hydrogen phosphate as the phosphorus source, with specific addition amounts as shown in Table A5.

For each solution, 2 mL of Stock1, 20 mL of Stock2, 2 mL of Stock3, 1 mL of Stock4, and 1 mL of Stock5 were mixed and dissolved in a 1000 mL volumetric flask and made up to volume. The resulting solutions were transferred to wide-mouth bottles and stored at 4 °C. These solutions constitute the phosphate concentration gradient media, labeled as A1, A2, A3, ..., A8. The phosphate concentrations in these media are shown in Table A6. The nitrogen (N) concentration in the media was maintained significantly higher than the upper limit threshold required for algal growth, ensuring an excess supply of nitrogen during algal growth.

Table A4. The formulations for the stock solutions.

Stock Solution	Preparation Method
Stock1	0.30 g C ₆ H ₈ O ₇ , 0.30 g C ₆ H ₈ FeNO ₇ , 0.050 g EDTANa ₂ , Dissolve and make up to 100 mL in a volumetric flask.
Stock2	30.0 g NaNO ₃ , 0.78 g K ₂ HPO ₄ , 1.50 g MgSO ₄ ·7H ₂ O, Dissolve and make up to 1000 mL in a volumetric flask.
Stock3	1.90 g CaCl ₂ ·2H ₂ O, Dissolve and make up to 100 mL in a volumetric flask.
Stock4	2.00 g Na ₂ CO ₃ , Dissolve and make up to 100 mL in a volumetric flask.
Stock5	2.860 g H ₃ BO ₃ , 1.8100 g MnCl ₂ ·4H ₂ O, 0.2220 g ZnSO ₄ ·7H ₂ O, 0.3910 g Na ₂ MoO ₄ , 0.0790 g CuSO ₄ ·5H ₂ O, 0.0490 g Co(NO ₃) ₂ ·6H ₂ O, Dissolve and make up to 1000 mL in a volumetric flask.

Table A5. Amount of potassium dihydrogen phosphate added.

P gradient Stock Solution	Amount of K ₂ HPO ₄ to Be Added (in Grams)
a1	0.01
a2	0.02
a3	0.04
a4	0.06
a5	0.1
a6	0.3
a7	0.6
a8	0.78

Table A6. Phosphorus concentration gradient.

Phosphorus Concentration Gradient Culture Medium	P Concentration (mg/L)
A1	0.03557
A2	0.07114
A3	0.14228
A4	0.2134
A5	0.3557
A6	1.0671
A7	2.1342
A8	2.7745

Appendix A.3. Experimental Design

Taking *Chlorella vulgaris* as an example: The phosphate concentration gradient culture media A1–8 and the starvation culture medium were placed in an autoclave, with parameters set at 121 °C for 30 min for sterilization. After sterilization, they were cooled to room temperature in a sterile workspace. *C. vulgaris* cultures, previously grown in enriched media, were centrifuged to concentrate using a centrifuge with settings at 7000 rpm for 15 min. The concentrated *C. vulgaris* cultures were diluted in the starvation medium and inoculated, sealed with plastic film, and all these procedures were carried out in aseptic conditions. The cultures were then placed in a light incubator for 3 days of starvation culture. The light incubation conditions were set at a temperature of 25 °C, light intensity of 3500 Lux, and a light-dark cycle of 12 h:12 h.

After the starvation culture, *C. vulgaris* cultures were concentrated using a centrifuge and then inoculated into culture media A1–8 with a pH adjustment to around 8.5. Each group of culture media had two parallel experimental groups. The initial algal density was measured, and the cultures were sealed and placed in the light incubator for 7 days of continuous cultivation under the same conditions as described earlier. Samples were taken every 24 h, and their algal density was measured using a Count star cell counter. The specific procedure was as follows: The culture flasks were shaken, 1 mL of algal culture was transferred to a 1.5 mL centrifuge tube using a pipette, and the culture flask was immediately sealed and returned to the light incubator. In the centrifuge tube, 10 microliters of Lugol's reagent were added using a pipette, mixed thoroughly, and 20 microliters of the fixed algal culture were drawn from the centrifuge tube and added to the Count star cell counting plate from the semi-circular portion. The algal density was measured using the Count star cell counter, and five measurements were taken for each culture, continuously for seven days. The experimental procedures for *Microcystis aeruginosa* and *Microcystis wesenbergii* were the same as those for *C. vulgaris*.

Appendix B.

Appendix B.1. Specific Growth Rate of *M. aeruginosa*

The fitted plot of $\ln(\bar{X})$ for *M. aeruginosa* against time is presented in Figures A1–A8.

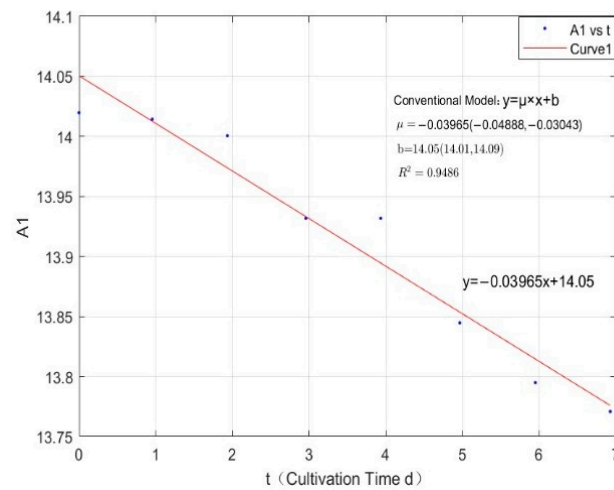


Figure A1. Fitted Plot for *M. aeruginosa* at Concentration A1.

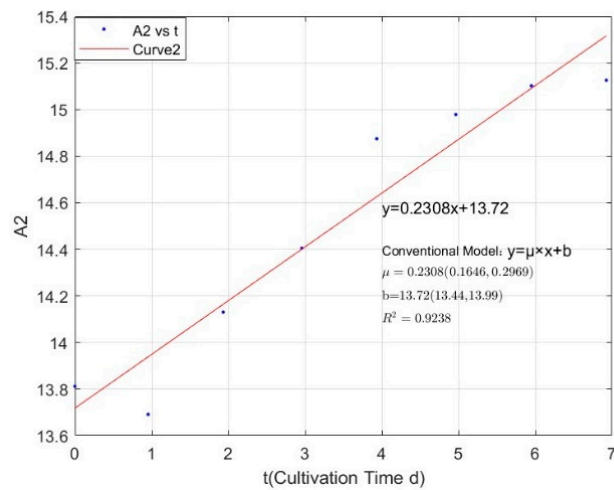


Figure A2. Fitted Plot for *M. aeruginosa* at Concentration A2.

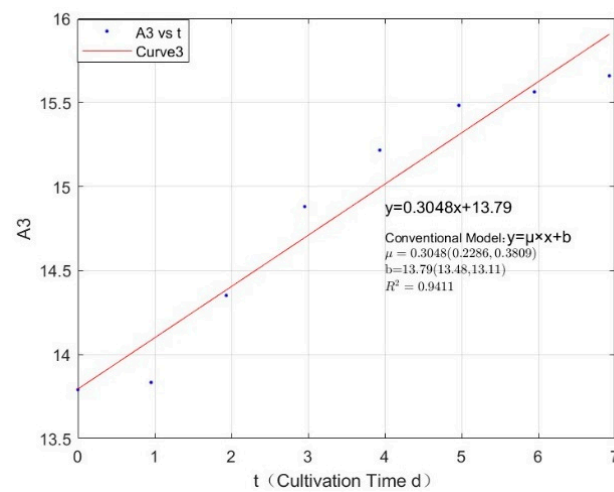


Figure A3. Fitted Plot for *M. aeruginosa* at Concentration A3.

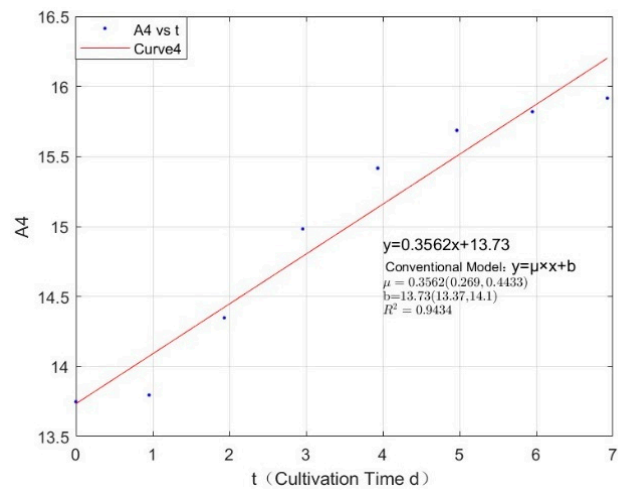


Figure A4. Fitted Plot for *M. aeruginosa* at Concentration A4.

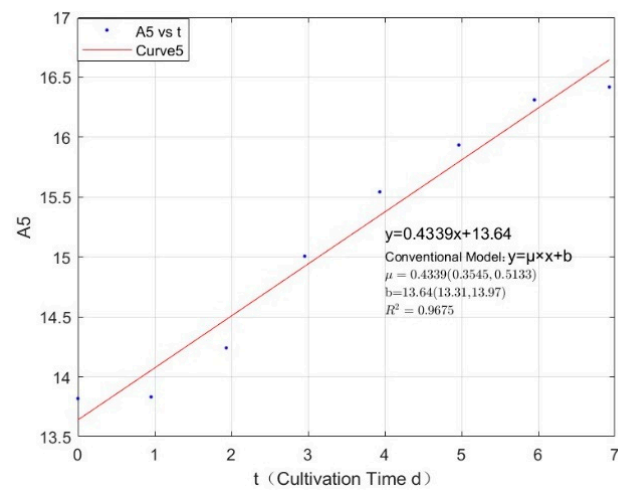


Figure A5. Fitted Plot for *M. aeruginosa* at Concentration A5.

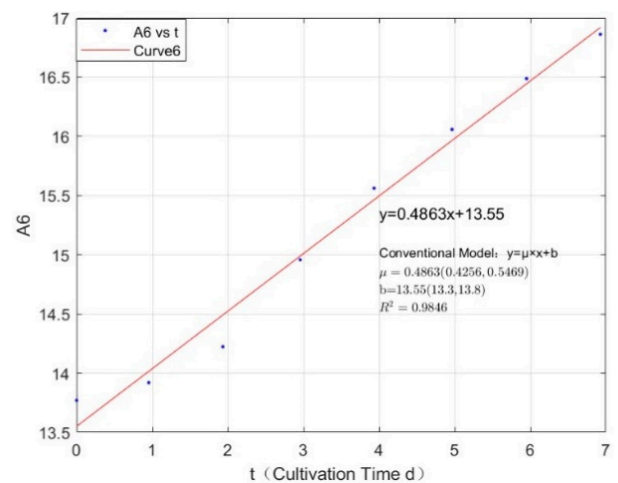


Figure A6. Fitting Plot for *M. aeruginosa* at Concentration A6.

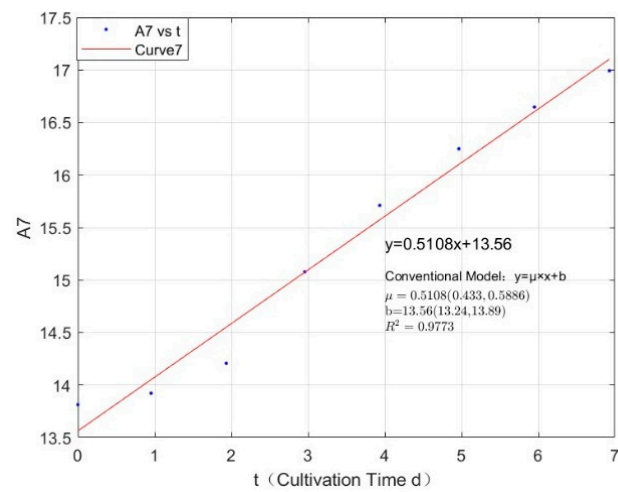


Figure A7. Fitted Plot for *M. aeruginosa* at Concentration A7.

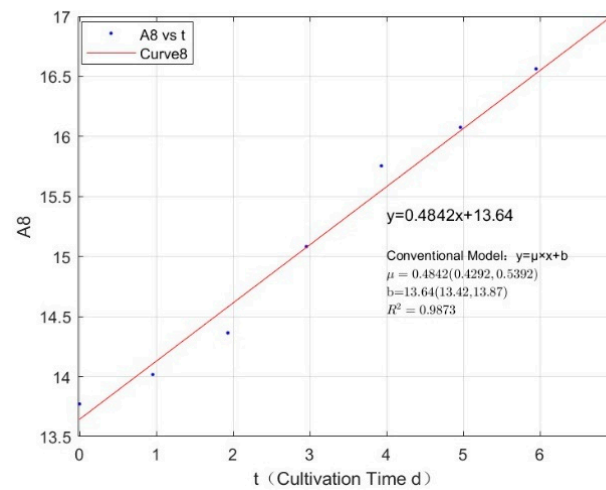


Figure A8. Fitted Plot for *M. aeruginosa* at Concentration A8.

The fitted plot of $\ln(\bar{X}_1, \bar{X}_2, \bar{X}_3)$ values of *M. aeruginosa* concerning for to time are shown in Figures A9–A16.

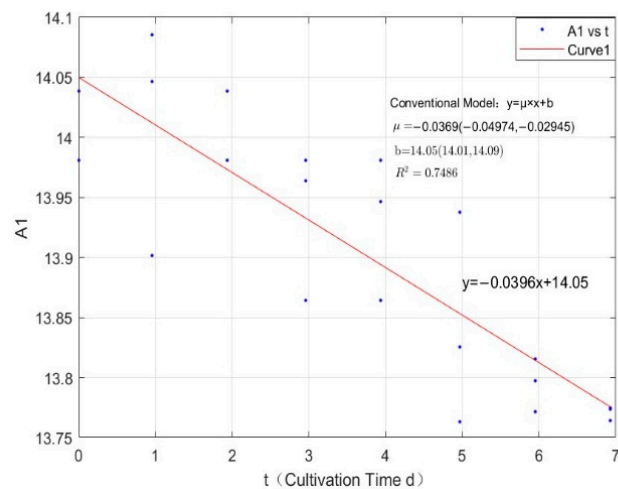


Figure A9. Fitted Plot for *M. aeruginosa* at Concentration A1.

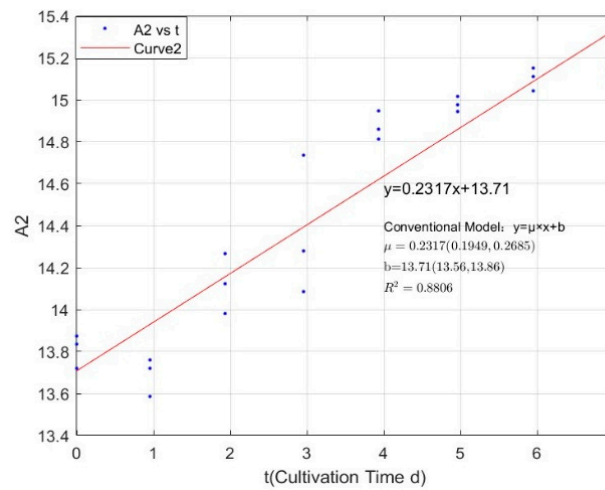


Figure A10. Fitted Plot for *M. aeruginosa* at Concentration A2.

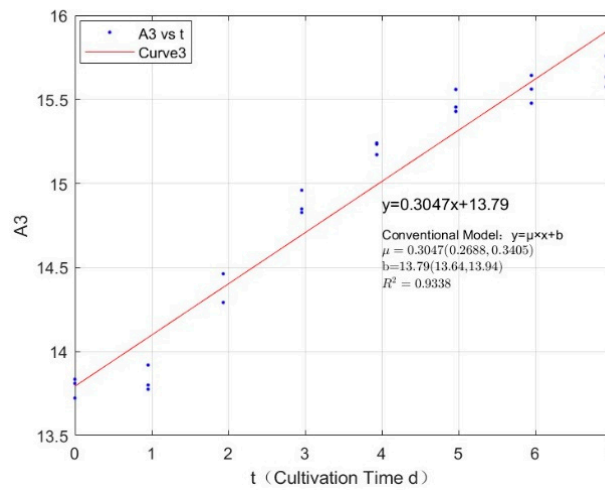


Figure A11. Fitted Plot for *M. aeruginosa* at Concentration A3.

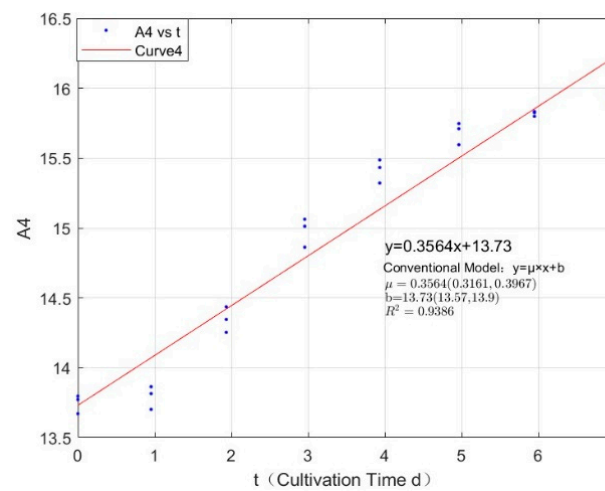


Figure A12. Fitted Plot for *M. aeruginosa* at Concentration A4.

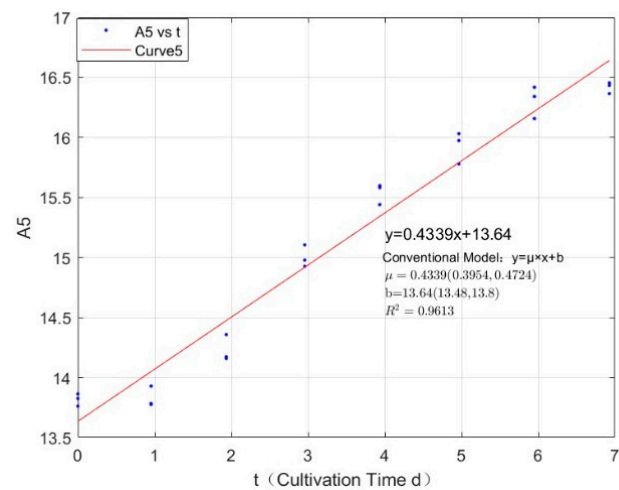


Figure A13. Fitted Plot for *M. aeruginosa* at Concentration A5.

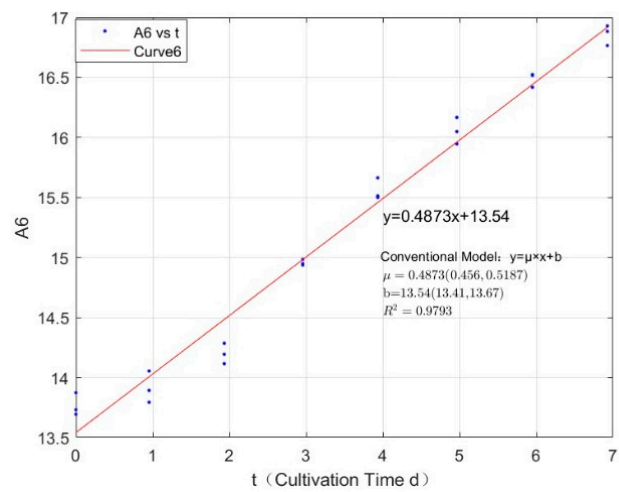


Figure A14. Fitted Plot for *M. aeruginosa* at Concentration A6.

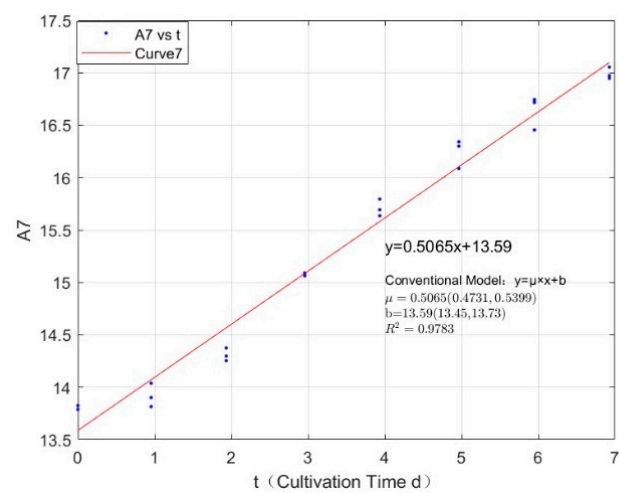


Figure A15. Fitted Plot for *M. aeruginosa* at Concentration A7.

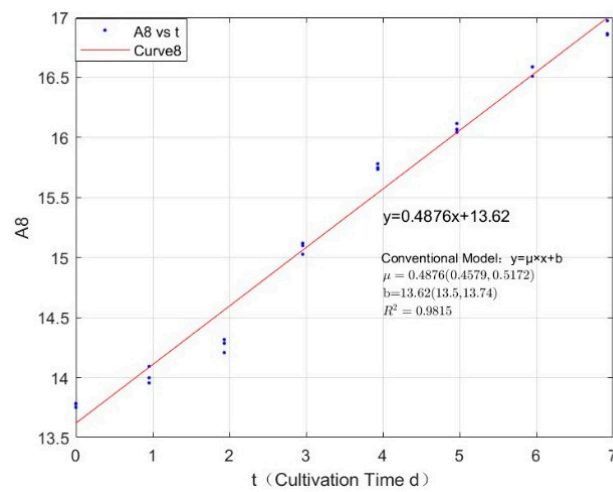


Figure A16. Fitted Plot for *M. aeruginosa* at Concentration A8.

Appendix B.2. Specific Growth Rate of *M. wesenbergii*

The fitted plot of $\ln(\bar{X})$ for *M. wesenbergii* against time is presented in Figures A17–A24.

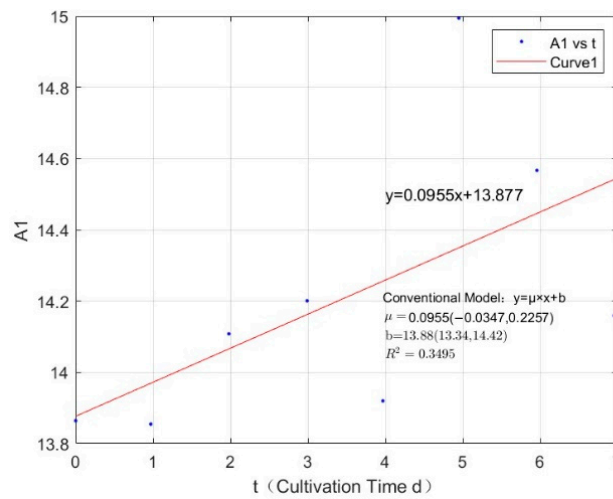


Figure A17. Fitted Plot for *M. wesenbergii* at Concentration A1.

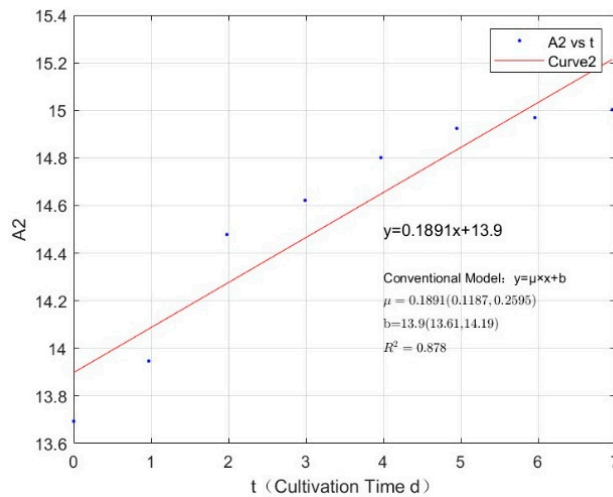


Figure A18. Fitted Plot for *M. wesenbergii* at Concentration A2.

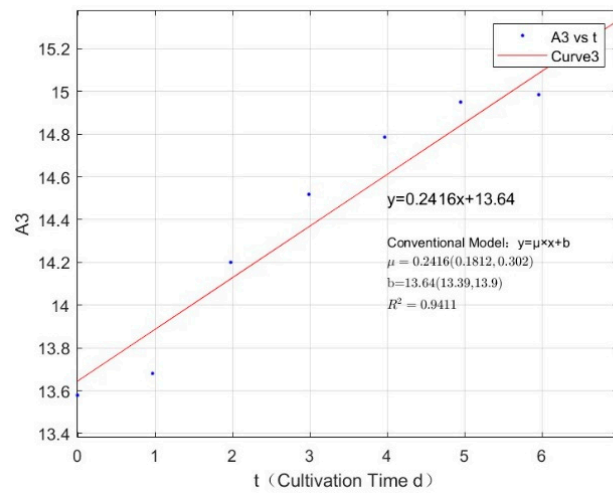


Figure A19. Fitted Plot for *M. wesenbergii* at Concentration A3.

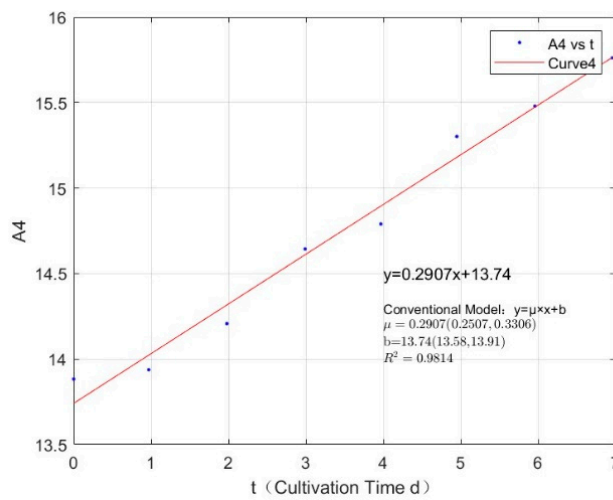


Figure A20. Fitted Plot for *M. wesenbergii* at Concentration A4.

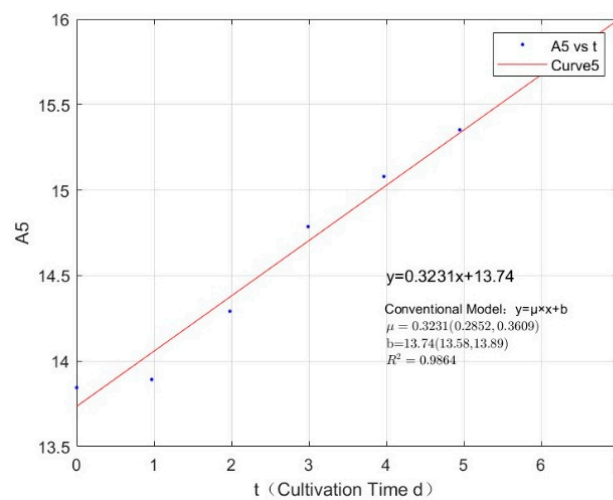


Figure A21. Fitted Plot for *M. wesenbergii* at Concentration A5.

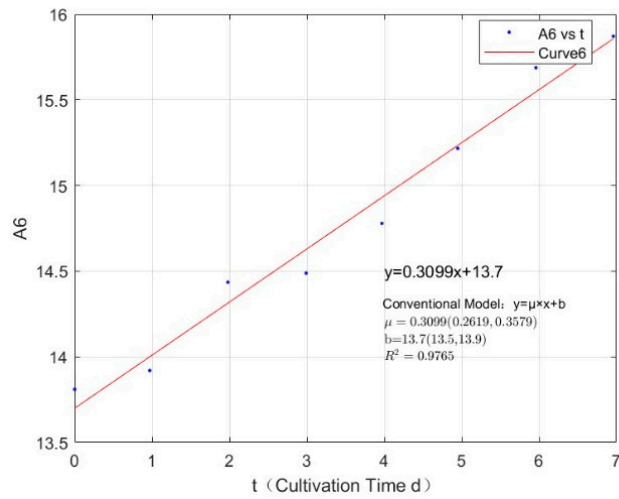


Figure A22. Fitted Plot for *M. wesenbergii* at Concentration A6.

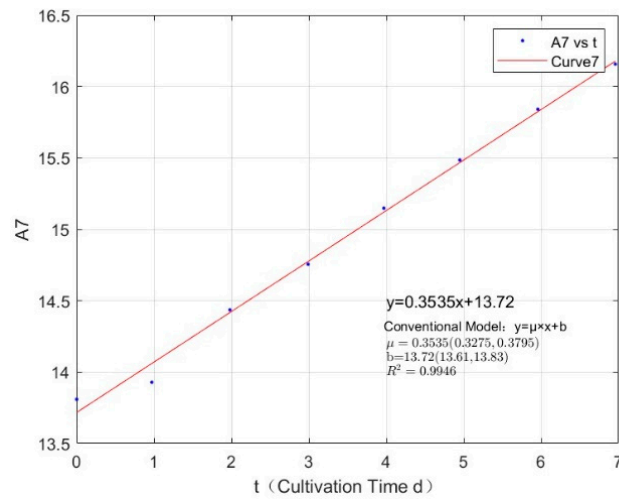


Figure A23. Fitted Plot for *M. wesenbergii* at Concentration A7.

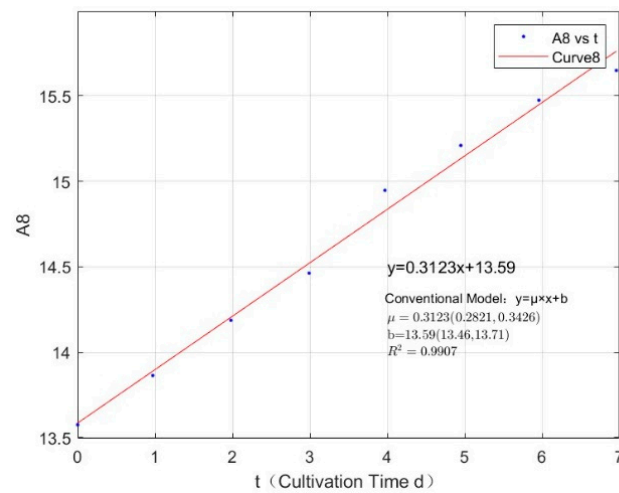


Figure A24. Fitted Plot for *M. wesenbergii* at Concentration A8.

The fitted plot of $\ln(\bar{X}_1, \bar{X}_2, \bar{X}_3)$ values of *M. wesenbergii* concerning for to time are shown in Figures A25–A32.

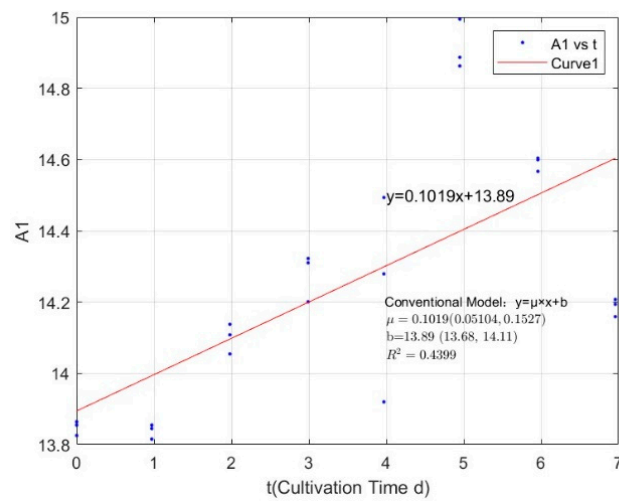


Figure A25. Fitted Plot for *M. wesenbergii* at Concentration A1.

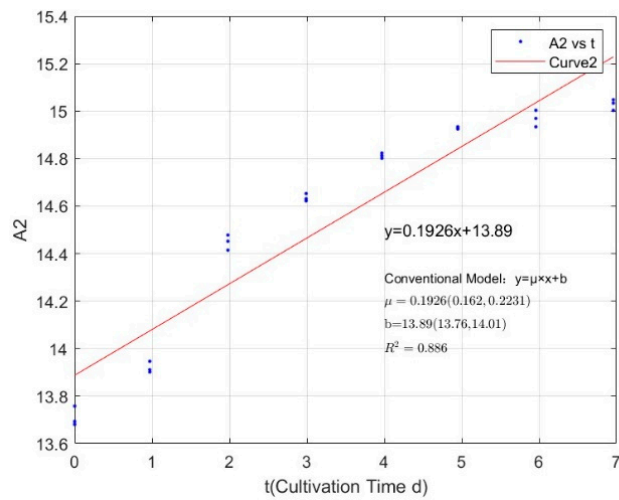


Figure A26. Fitted Plot for *M. wesenbergii* at Concentration A5.

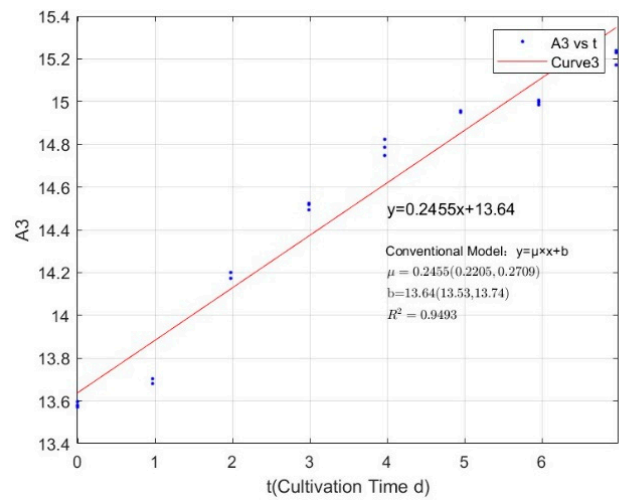


Figure A27. Fitted Plot for *M. wesenbergii* at Concentration A5.

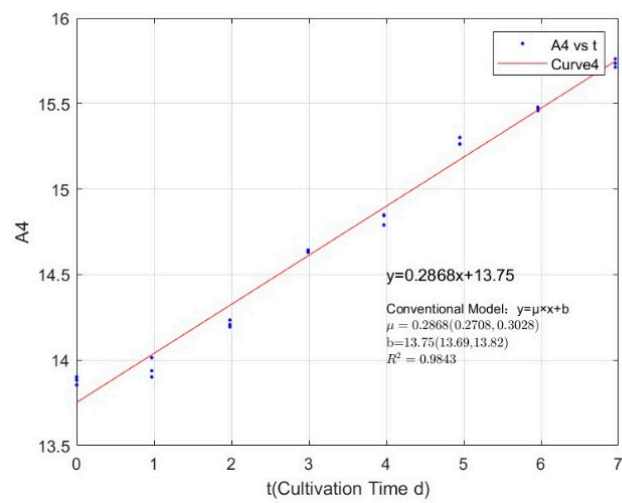


Figure A28. Fitted Plot for *M. wesenbergii* at Concentration A4.

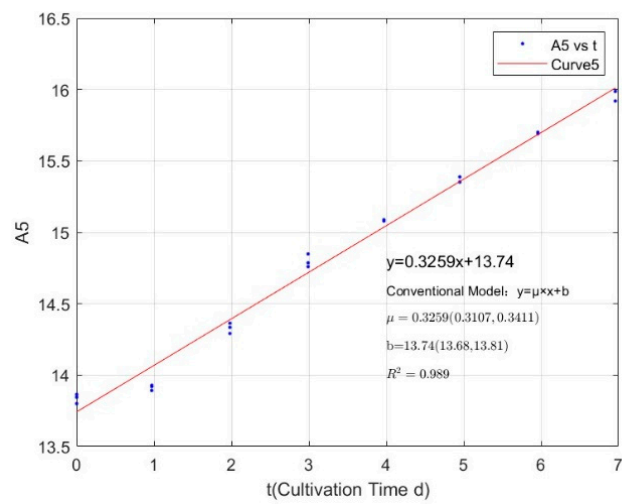


Figure A29. Fitted Plot for *M. wesenbergii* at Concentration A5.

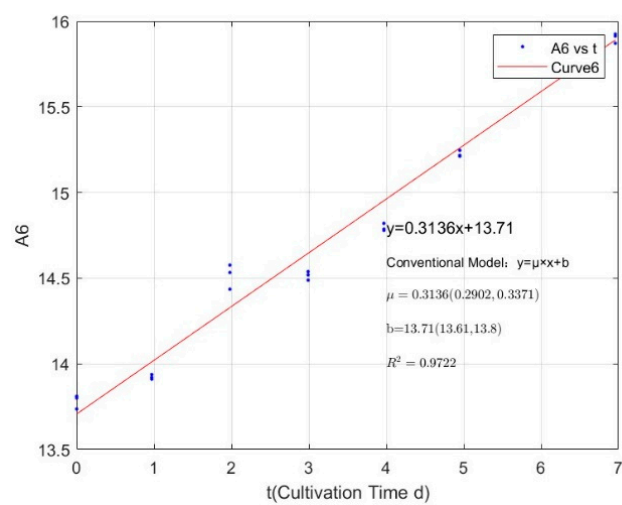


Figure A30. Fitted Plot for *M. wesenbergii* at Concentration A6.

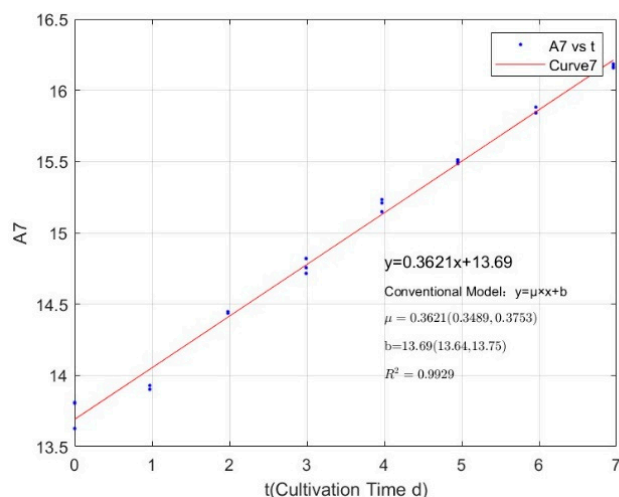


Figure A31. Fitted Plot for *M. wesenbergii* at Concentration A7.

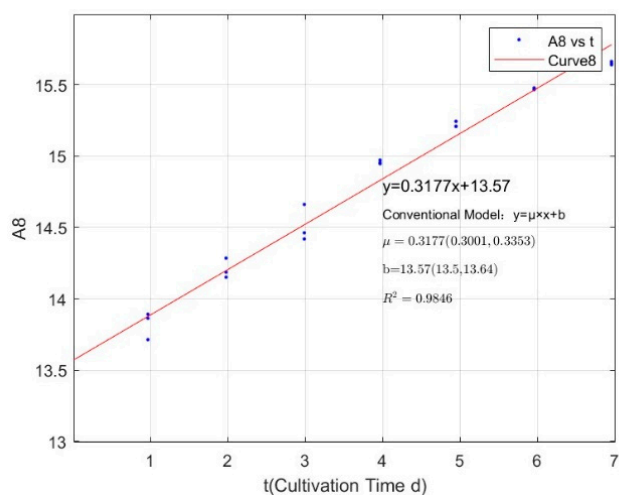


Figure A32. Fitted Plot for *M. wesenbergii* at Concentration A8.

References

- Xia, R.; Zhang, Y.; Wang, G.; Zhang, Y.; Dou, M.; Hou, X.; Qiao, Y.; Wang, Q.; Yang, Z. Multi-factor identification and modelling analyses for managing large river algal blooms. *Environ. Pollut.* **2019**, *254*, 113056. [[CrossRef](#)] [[PubMed](#)]
- Paerl, H.W.; Fulton, R.S., 3rd; Moisaner, P.H.; Dyble, J. Harmful freshwater algal blooms, with an emphasis on cyanobacteria. *Sci. World J.* **2001**, *1*, 76–113. [[CrossRef](#)] [[PubMed](#)]
- Yang, J.R.; Lv, H.; Isabwe, A.; Liu, L.; Yu, X.; Chen, H. Disturbance-induced phytoplankton regime shifts and recovery of cyanobacteria dominance in two subtropical reservoirs. *Water Res.* **2017**, *120*, 52–63. [[CrossRef](#)] [[PubMed](#)]
- Yang, Z.; Zhang, M.; Shi, X.; Kong, F.; Ma, R.; Yu, Y. Nutrient reduction magnifies the impact of extreme weather on cyanobacterial bloom formation in large shallow Lake Taihu (China). *Water Res.* **2016**, *103*, 302–310. [[CrossRef](#)] [[PubMed](#)]
- Koeller, P.; Fuentes-Yaco, C.; Platt, T.; Sathyendranath, S.; Richards, A.; Ouellet, P.; Orr, D.; Skúladóttir, U.; Wieland, K.; Savard, L.; et al. Basin-scale coherence in phenology of shrimps and phytoplankton in the North Atlantic Ocean. *Science* **2009**, *324*, 791–793. [[CrossRef](#)] [[PubMed](#)]
- Metsoviti, M.N.; Katsoulas, N.; Karapanagiotidis, I.T.; Papapolymerou, G. Effect of nitrogen concentration, two-stage and prolonged cultivation on growth rate, lipid and protein content of *Chlorella vulgaris*. *J. Chem. Technol. Biotechnol.* **2019**, *94*, 1466–1473. [[CrossRef](#)]
- Lehtola, M.J.; Miettinen, I.T.; Keinänen, M.M.; Kekki, T.K.; Laine, O.; Hirvonen, A.; Vartiainen, T.; Martikainen, P.J. Microbiology, chemistry and biofilm development in a pilot drinking water distribution system with copper and plastic pipes. *Water Res.* **2004**, *38*, 3769–3779. [[CrossRef](#)]
- Chokshi, K.; Pancha, I.; Ghosh, A.; Mishra, S. Nitrogen starvation-induced cellular crosstalk of ROS-scavenging antioxidants and phytohormone enhanced the biofuel potential of green microalga *Acutodesmus dimorphus*. *Biotechnol. Biofuels* **2017**, *10*, 60. [[CrossRef](#)]

9. Lee, T.A.; Rollwagen-Bollens, G.; Bollens, S.M. The influence of water quality variables on cyanobacterial blooms and phytoplankton community composition in a shallow temperate lake. *Environ. Monit. Assess.* **2015**, *187*, 315. [[CrossRef](#)]
10. O'Neil, J.M.; Davis, T.W.; Burford, M.A.; Gobler, C.J. The rise of harmful cyanobacteria blooms: The potential roles of eutrophication and climate change. *Harmful Algae* **2012**, *14*, 313–334. [[CrossRef](#)]
11. Smith, V.H. Eutrophication of freshwater and coastal marine ecosystems a global problem. *Environ. Sci. Pollut. Res.* **2003**, *10*, 126–139. [[CrossRef](#)] [[PubMed](#)]
12. Chen, Y.; Qin, B.; Teubner, K.; Dokulil, M.T. Long-term dynamics of phytoplankton assemblages: Microcystis-domination in Lake Taihu, a large shallow lake in China. *J. Plankton Res.* **2003**, *25*, 445–453. [[CrossRef](#)]
13. Yan, K.; Xu, J.-C.; Gao, W.; Li, M.-J.; Yuan, Z.-W.; Zhang, F.-S.; Elser, J. Human perturbation on phosphorus cycles in one of China's most eutrophicated lakes. *Resour. Environ. Sustain.* **2021**, *4*, 100026. [[CrossRef](#)]
14. Redfield, A.C. The biological control of chemical factors in the environment. *Am. Sci.* **1958**, *46*, 230A–221.
15. Liebig, J.V. *Die Organische Chemie in Ihrer Anwendung Auf Agricultur Und Physiologie*; Springer: Berlin/Heidelberg, Germany, 1841.
16. Caperon, J. Population growth in micro-organisms limited by food supply. *Ecology* **1967**, *48*, 715–722. [[CrossRef](#)] [[PubMed](#)]
17. Morrison, K.; Thérien, N.; Marcos, B. Comparison of six models for nutrient limitations on phytoplankton growth. *Can. J. Fish. Aquat. Sci.* **1987**, *44*, 1278–1288. [[CrossRef](#)]
18. Zhao, G.; Gao, X.; Zhang, G.; Sang, G. The effects of turbulence on phytoplankton and implications for energy transfer with an integrated water quality-ecosystem model in a shallow lake. *J. Environ. Manag.* **2020**, *256*, 109954. [[CrossRef](#)]
19. Liu, Y.; Xin, Y.; Li, R.; Xin, Q.; Lin, X. Mechanisms and Countermeasures for the Outbreak of Cyanobacterial Blooms in Lake Taihu. *Lake Sci.* **2019**, *31*, 18–27.
20. Zhang, M.; Shi, X. The variation of water quality from 2012 to 2018 in Lake Chaohu and the mitigating strategy on cyanobacterial blooms. *J. Lake Sci.* **2020**, *32*, 11–20.
21. Zhao, H.; Li, J.; Yan, X.; Fang, S.; Du, Y.; Xue, B.; Yu, K.; Wang, C. Monitoring Cyanobacteria Bloom in Dianchi Lake Based on Ground-Based Multispectral Remote-Sensing Imaging: Preliminary Results. *Remote Sens.* **2021**, *13*, 3970. [[CrossRef](#)]
22. Zhu, G.; Qin, B.-Q.; Zhang, Y.; Xu, H. Variation and driving factors of nutrients and chlorophyll-a concentrations in northern region of Lake Taihu, China, 2005–2017. *J. Lake Sci.* **2018**, *30*, 279–295.
23. Xu, H.; Paerl, H.W.; Qin, B.; Zhu, G.; Gao, G. Nitrogen and phosphorus inputs control phytoplankton growth in eutrophic Lake Taihu, China. *Limnol. Oceanogr.* **2010**, *55*, 420–432. [[CrossRef](#)]
24. Wu, Y.; Xu, H.; Yang, G.; Zhu, G.; Qin, B. Developing the critical phosphorus threshold for spring algal growth in Lake Taihu, China. *China Environ. Sci.* **2013**, *33*, 1622–1629.
25. Xu, H.; Paerl, H.W.; Qin, B.; Zhu, G.; Hall, N.S.; Wu, Y. Determining critical nutrient thresholds needed to control harmful cyanobacterial blooms in eutrophic Lake Taihu, China. *Environ. Sci. Technol.* **2015**, *49*, 1051–1059. [[CrossRef](#)] [[PubMed](#)]
26. Xu, H.; Paerl, H.W.; Zhu, G.; Qin, B.; Hall, N.S.; Zhu, M. Long-term nutrient trends and harmful cyanobacterial bloom potential in hypertrophic Lake Taihu, China. *Hydrobiologia* **2017**, *787*, 229–242. [[CrossRef](#)]
27. Vollenwelder, R.A.; Janus, L.L. *OECD Cooperative Programme on Eutrophication*; Citeseer; Environment Canada: Burlington, ON, Canada, 1981.
28. Gibson, G.; Carlson, R.; Simpson, J.; Smeltzer, E.; Kennedy, R. *Nutrient Criteria Technical Guidance Manual Lake and Reservoirs*; United States Environmental Protection Agency: Washington, DC, USA, 2000.
29. Monod, J. The growth of bacterial cultures. *Annu. Rev. Microbiol.* **1949**, *3*, 371–394. [[CrossRef](#)]
30. Chen, L.-M.; Chai, L.-H. Mathematical model and mechanisms for biofilm wastewater treatment systems. *World J. Microbiol. Biotechnol.* **2005**, *21*, 1455–1460. [[CrossRef](#)]
31. Rittmann, B.E.; McCarty, P.L. *Environmental Biotechnology: Principles and Applications*; McGraw-Hill Education: New York, NY, USA, 2001.
32. Ketchum, B.H. The absorption of phosphate and nitrate by illuminated cultures of *Nitzschia closterium*. *Am. J. Bot.* **1939**, *26*, 399–407. [[CrossRef](#)]
33. Ketchum, B.H. The development and restoration of deficiencies in the phosphorus and nitrogen composition of unicellular plants. *J. Cell. Comp. Physiol.* **1939**, *13*, 373–381. [[CrossRef](#)]
34. Aitchison, P.; Butt, V. The relation between the synthesis of inorganic polyphosphate and phosphate uptake by *Chlorella vulgaris*. *J. Exp. Bot.* **1973**, *24*, 497–510. [[CrossRef](#)]
35. Albi, T.; Serrano, A. Inorganic polyphosphate in the microbial world. Emerging roles for a multifaceted biopolymer. *World J. Microbiol. Biotechnol.* **2016**, *32*, 27. [[CrossRef](#)] [[PubMed](#)]
36. Caperon, J. Population growth response of *Isochrysis galbana* to nitrate variation at limiting concentrations. *Ecology* **1968**, *49*, 866–872. [[CrossRef](#)]
37. Fuhs, G.W. Phosphorus content and rate of growth in the diatoms *Cyclotella nana* and *Thalassiosira fluviatilis*. *J. Phycol.* **1969**, *5*, 312–321. [[CrossRef](#)] [[PubMed](#)]
38. Rhee, G.Y. A continuous culture study of phosphate uptake, growth rate and polyphosphate in *Scenedesmus* sp. 1. *J. Phycol.* **1973**, *9*, 495–506. [[CrossRef](#)]
39. Chu, F.-F.; Chu, P.-N.; Cai, P.-J.; Li, W.-W.; Lam, P.K.; Zeng, R.J. Phosphorus plays an important role in enhancing biodiesel productivity of *Chlorella vulgaris* under nitrogen deficiency. *Bioresour. Technol.* **2013**, *134*, 341–346. [[CrossRef](#)] [[PubMed](#)]

40. Xiao, P.; Qing, S.; Jin, G.; Yong, W.P. Research Progress on the Effects of Inorganic Phosphorus on Plant Leaf Photosynthesis and Its Mechanisms. *J. Plant Nutr. Fertil.* **1997**, *3*, 201–208.
41. Yin, C.; Liang, Y.; Zhang, Q. Effects of Nitrogen Concentration on Chlorophyll Fluorescence Characteristics and Growth of *Chlorella vulgaris* 3011 and 8701. *Fish. Sci.* **2008**, *27*, 27–31.
42. Sun, Y. The Effects of Fe³⁺ on the Growth and Lipid Content of *Chlorella*. *Biotechnol. Bull.* **2014**, *4*, 181.

Disclaimer/Publisher's Note: The statements, opinions and data contained in all publications are solely those of the individual author(s) and contributor(s) and not of MDPI and/or the editor(s). MDPI and/or the editor(s) disclaim responsibility for any injury to people or property resulting from any ideas, methods, instructions or products referred to in the content.